CHALMERS
UNIVERSITY OF TECHNOLOGY

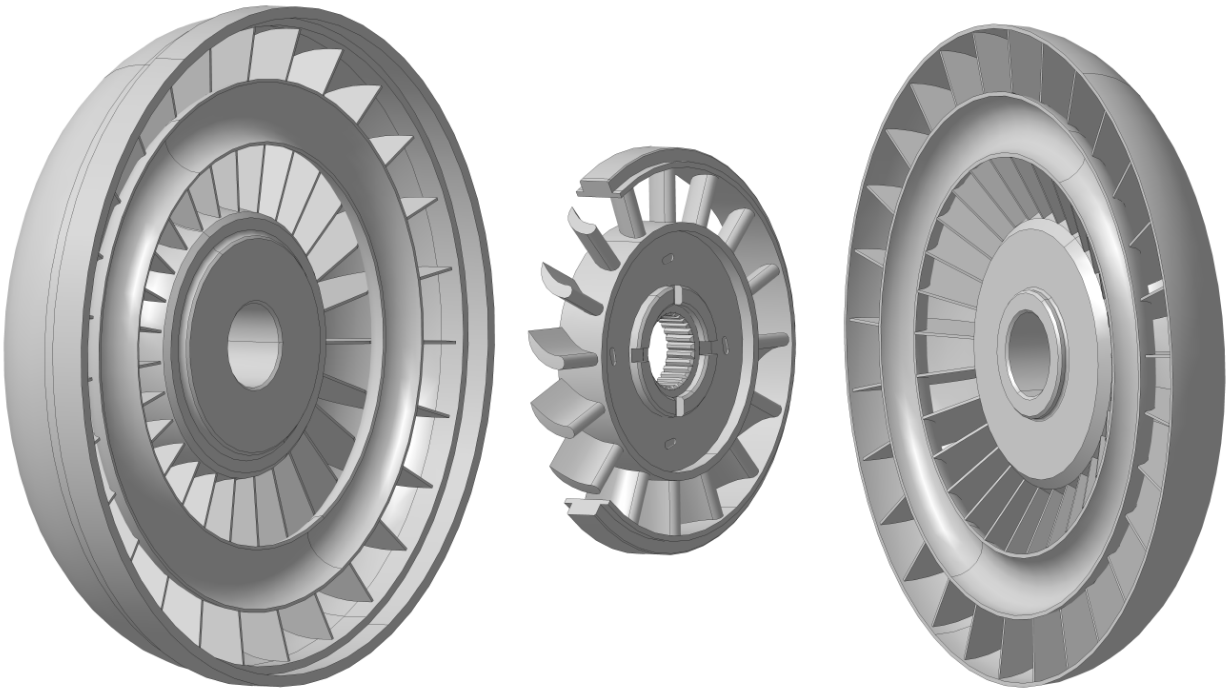

Modelling and measurement of transient torque converter characteristics

Master's thesis in Automotive Engineering

YANG LI
MAX SUNDÉN

Department of Applied Mechanics
CHALMERS UNIVERSITY OF TECHNOLOGY
Gothenburg, Sweden 2016

Master's thesis in automotive engineering

Modelling and measurement of transient torque converter characteristics

YANG LI
MAX SUNDÉN

CHALMERS
UNIVERSITY OF TECHNOLOGY

Department of Applied Mechanics
Division of Vehicle Engineering & Autonomous Systems
Vehicle Dynamics Group
Chalmers University of Technology
Gothenburg, Sweden 2016

Modelling and measurement of transient torque converter characteristics
YANG LI
MAX SUNDÉN

Examiner: Professor Bengt J H Jacobson, Chalmers University of Technology
Supervisor: Fredrik Henningsson, Volvo Car Corporation

Master's Thesis 2016:74
ISSN 1652-8557
Department of Applied Mechanics
Division of Vehicle Engineering & Autonomous Systems
Vehicle Dynamics Group
Chalmers University of Technology
SE-412 96 Gothenburg
Telephone +46 31 772 1000

Cover: A three-element torque converter.

Gothenburg, Sweden 2016

Modelling and measurement of transient torque converter characteristics
YANG LI
MAX SUNDÉN
Department of Applied Mechanics
Chalmers University of Technology

Abstract

The torque converter is a crucial component in the drivetrain of a vehicle equipped with an automatic gearbox. It has the ability to transfer power with torque amplification, allow slip between engine and transmission and dampen vibrations between the two. For these reasons its characteristics will have a direct effect on the vehicle's performance, fuel economy, drivability and comfort. The behaviour of the torque converter is often modelled based on standardised component testing in the form of measured steady-state performance. It is however known that transient dynamics can have a significant impact under certain conditions, such as vehicle take-off.
In order to aid the development of high quality products it is desired to predict component behaviour with as high accuracy as possible. For a vehicle manufacturer such as Volvo Cars, it is usually of higher importance to accurately capture real-world driving conditions and to specify performance targets that can be linked to customer sensation rather than mechanical properties.
In this thesis, transient simulation models based on steady-state measurements, used at Volvo Cars were evaluated against measurement data to investigate if they could be parameterised to simulate the behaviour of other torque converters, even under transient conditions. A model based on hardware parameters rather than measured behaviour was also implemented and evaluated.

Keywords: Torque converter, automatic transmission, dynamic, transient, launch, take-off, startability, drivability, simulation, modelling.

Acknowledgements

First of all we would like to thank or supervisors Mr. Fredrik Henningsson and Mr. Gabriel Palmenäs from the Volvo Car Corporation for providing us with the opportunity to study this interesting subject and for having confidence in us. We would also like to thank our examiner Mr. Bengt J H Jacobson from the Chalmers University of Technology for his guidance and support. The three were always available for discussions, to give their support and to share their knowledge in everything from technical questions to methodology, structure and writing.

We would also like to thank the colleagues at *97122 - Powertrain Strategy & Concept* for their encouragement and support during our time in the group, for troubleshooting and support in VSIM and DYMOLA and for excellent fika. Lastly, we would also like to acknowledge Mr. Mikael Törmänen and Mr. Edo Drenth as well as the staff at *97730 - Automatic Gearbox, 97544 - Combustion Control Diesel, 97545 - Combustion Control Petrol, 91915 - Powertrain Workshop and 91844 - Metrology and Fuel Distribution* for input, technical support and help in general!

Yang Li and Max Sundén, Gothenburg, 2016

Contents

1
Introduction

1.1 Background

The torque converter is a crucial component in the drivetrain of a vehicle equipped with an automatic gearbox. It has the ability to transfer power with torque amplification, allow slip between engine and transmission and dampen vibrations between the two. For these reasons its characteristics will have a direct effect on the vehicle's performance, fuel economy, drivability and comfort.
The behaviour of the torque converter is often modelled based on measured steady-state performance, since this is relatively easy to measure and therefore readily available from the manufacturers. It is however known that transient dynamics can have a significant impact under certain conditions, such as vehicle take-off [2].
Steady-state testing does not take inertia of the components nor the working fluid inside the torque converter into account and is therefore not able to capture transient behaviour. Another problem that arises with this type of modelling is that it is based on performance measurements, i.e. a physical torque converter is needed. For this reason such models cannot be used in the early phases of development, e.g. to evaluate design concepts.
The torque converter simulation models currently used at Volvo Cars are based on steady-state measurements, but also employ different strategies to compensate for transient effects. They are however not thoroughly verified for transient conditions.

1.2 Objectives

In order to aid the development of high quality products it is desired to predict component behaviour with as high accuracy as possible. For the reasons mentioned above in Section 1.1, the Volvo Car Corporation is interested in the development of a simulation model with the capability to capture the torque converters transient performance under real world driving conditions. It is also desirable to build a model based on hardware design parameters, which will give the ability to predict the behaviour of different torque converter concepts without the need of physical prototypes.
Volvo Cars currently use an in-house developed simulation tool called VSIM - Vehicle Simulation Tool, for complete vehicle simulation. VSIM is based on MATLAB and Simulink.

1.3 Limitations

1. The torque converter stator operates under two different modes; freewheeling or locked. Since the aim of this thesis is to examine transient dynamics, modelling will only include the locked stator mode.
2. The torque converter lock-up clutch operates under three different modes; open, slipping or locked. Analogue to the above reasoning, modelling will only include open lock-up clutch.

These limitations will be further elaborated and explained in the following chapter.

2

Theory

2.1 Torque converter basics

2.1.1 The two-element fluid coupling

The hydrodynamic torque converter is based on the two-element fluid coupling.

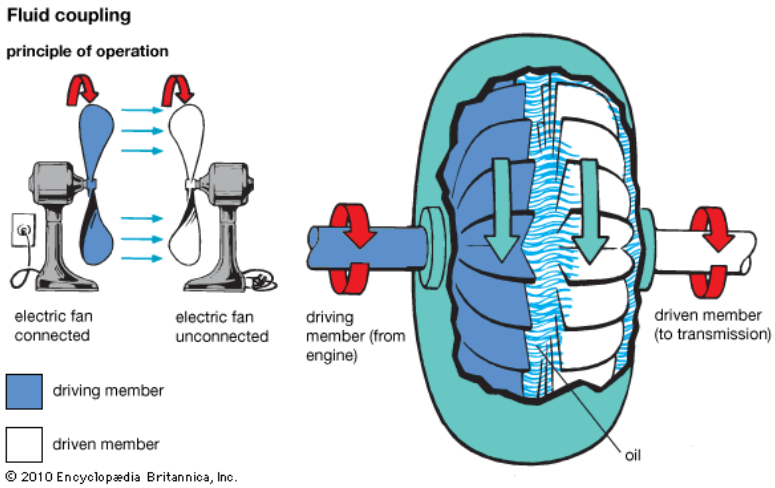

By courtesy of Encyclopaedia Britannica, Inc., copyright 2010; used with permission.

Figure 2.1: Two-element fluid coupling.

The operation of the two-element fluid coupling can be thought of as two opposing desk fans, as seen in Figure 2.1. When the driving fan is accelerated it will cause air to flow over the blades of the driven fan, thereby causing it too to rotate and hence transferring power. The fluid coupling operates using the very same principle, but instead of air it typically employs oil as the working medium. The two sets of blades are typically encapsulated inside a housing, such that the working media can re-circulate in a closed loop. The driving member is called the *pump* or *impeller* and the driven member is called the

turbine. In automotive applications the impeller is directly connected to the output shaft of the engine and the turbine is directly connected to the input shaft of the transmission. Because of losses there will always be a degree of slip between the two elements when torque is transferred, i.e. the rotational speed of the driving member will always be greater than the rotational speed of the driven member. The relationship between these speeds is an important parameter when describing the behaviour of a fluid coupling. A practical and common way of describing this relationship is to divide the rotational speed of the output by the rotational speed of the input, usually denoted the *Speed Ratio, SR*:

$$SR = \omega_{output}/\omega_{input} \tag{2.1}$$

or, which will be used throughout this thesis;

$$SR = \omega_{turbine}/\omega_{impeller} \tag{2.2}$$

Since the fluid coupling has the ability to slip, i.e. impeller and turbine can operate at individual rotational speeds, it is possible to keep the engine running while holding the vehicle stationary, for instance by applying the brakes. At this point the Speed Ratio is obviously zero. As the brakes are released and the throttle applied the impeller will accelerate and transfer power to the fluid which in turn will transfer it to the turbine thereby causing it to rotate and hence the vehicle to accelerate. The working fluid enters the rotating impeller near the centre axis, where the tangential component of the absolute velocity is low. By guiding of the shell and blades and by the rotation of the impeller, the fluid is then forced radially outwards to where the tangential component of the absolute velocity is high, thereby gaining kinetic energy. The fluid then enters the turbine, where it is guided back towards the centre, thereby transferring kinetic energy to the turbine wheel. The fluid then re-enters the impeller, but since it has transferred power to the turbine, it does so at a lower velocity, thereby braking the speed of the impeller. This drawback is solved by introducing a third element, called *stator* or *reactor*, in the flow path between the turbine and the impeller.

2.1.2 The three-element torque converter

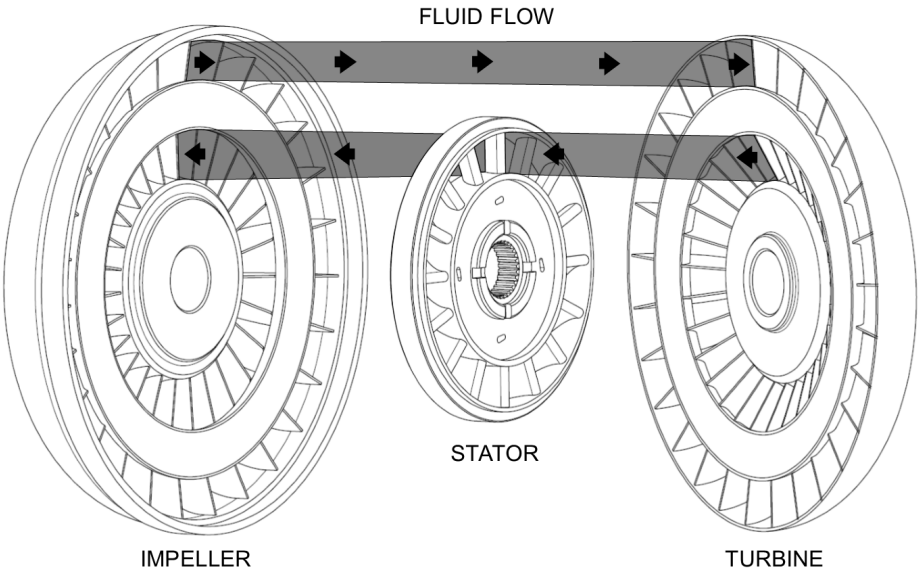

Figure 2.2: Three-element torque converter.

The *stator*, sometimes also called the *reactor*, is what differentiates the torque converter from the two-element fluid coupling. It is located in the flow path between the turbine and the impeller and redirects the flow in the direction of rotation.

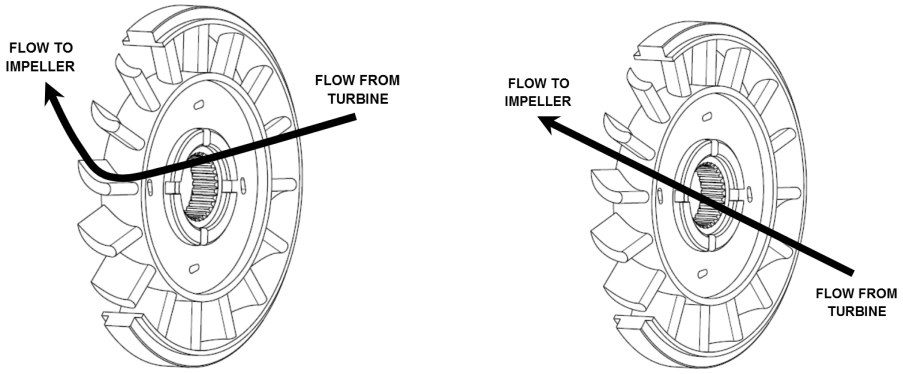

(a) Low Speed Ratio **(b)** High Speed Ratio

Figure 2.3: Flow paths through the stator.

At stall and at low speed ratios, such as the early phase of acceleration, the flow through the stator will follow the path in Figure 2.3a. The flow will impact the front-side of the stator blades, thereby imparting a torque on the stator (counter-clockwise in Figure 2.3a). However the stator is mounted to the torque converter housing via a one-way clutch which only allows the stator to rotate in the same direction as the torque converter itself (clockwise in Figure 2.3a). In this case the stator will therefore be stationary, hence the name. Moreover the stator's blading will direct the flow in the same direction as the rotation of the impeller. This gives the torque converter the ability to amplify torque, something that the two-element fluid coupling can not. If torque is defined as positive when it attempts to produce rotation in the same direction as engine rotation, then (at stall and low speed ratios):

- Impeller torque is negative (reaction to engine torque)
- Turbine torque is positive (rotation in same direction as engine rotation)
- Stator torque is negative (rotation in opposite direction as engine rotation)

Since these three torques are the only ones acting on the torque converter, the following must hold true:

$$-T_{impeller} + T_{turbine} - T_{stator} = 0 \tag{2.3}$$

Which can be rearranged as:

$$T_{turbine} = T_{impeller} + T_{stator} \tag{2.4}$$

This shows the effect of torque amplification at stall and low speed ratios; the turbine torque is the sum of the impeller torque and the stator torque. Analogue to the Speed Ratio, this ability to amplify torque is commonly denoted the *Torque Ratio, TR*:

$$TR = T_{output}/T_{input} \tag{2.5}$$

or, which will be used throughout this thesis:

$$TR = T_{turbine}/T_{impeller} \tag{2.6}$$

This torque amplification does however have its limitations. The flow inside the torque converter can be divided into two components: radial and axial. To achieve a high torque amplification, a large axial flow through the stator and a large deflection of the fluid is necessary, since this is what creates

the stator torque. The axial flow is shown in Figure 2.2 and 2.3 and will peak when the converter is at stall. As the turbine accelerates (Speed Ratio increases) the flow inside the converter will progressively change to radial. High slip is a necessity for high torque amplification, since power is the product of torque and speed. This it what gives the torque *converter* its name; any increase in torque can only by accomplished by a decrease in speed (for a given input power). High torque amplification is also a function of large flow redirection and in this process some of the fluids kinetic energy will be converted to heat by friction and turbulence.
The efficiency of a torque converter can be calculated as:

$$\eta = TR \cdot SR \tag{2.7}$$

From the above equation it can be noted that the higher the stall Torque Ratio is, the steeper the initial slope of the efficiency curve will be. The figure below shows the efficiency curve for two different torque converters and illustrates the trend of how torque amplification affects efficiency.

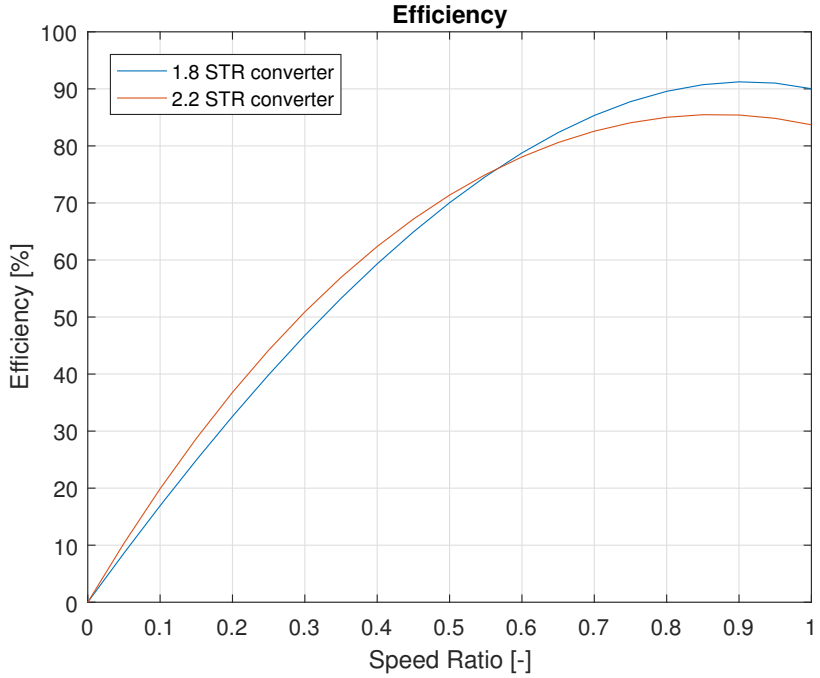

Figure 2.4: Efficiency plot for two torque converters (free-wheeling stator, open lock-up). STR = Stall Torque Ratio.

The higher the Stall Torque Ratio is, the more efficient the converter will typically be a low speed ratios. However, this also leads to lower peak efficiency and lower efficiency at high speed ratios.
A modern torque converter for passenger car applications typically has a stall Torque Ratio of about 2, meaning that it has the capability to double output torque [5]. Higher amplification is possible, but as shown above leads to lower peak and high Speed Ratio efficiency and for these reasons most manufacturers seem to opt for the 1.8-2.2 range [5]. Early torque converter designs typically had higher torque amplification, but with ever increasing demands on fuel consumption, efficiency has been prioritised and since modern gear boxes typically have a higher number of gears the need for high amplification in the torque converter has decreased.
As the turbine picks up speed the flow angle between the turbine and the stator will change. At a certain point, typically around $SR = 0.85$, the flow will start to impact the back-side of the stator blades, as shown in Figure 2.3b. At this point the torque on the stator will change sign and because of the one-way clutch the stator will now begin to rotate in the same direction as the other components. The Speed Ratio at which this transition takes place is called the *coupling point*. By changing the sign of the stator torque in Equation 2.4, the benefit of the one-way clutch should be clear; without it the output torque would always be lower than the input torque above the coupling point. Above this Speed Ratio the stator is free-wheeling to decrease losses and the torque converter is no longer capable of providing torque amplification.
The three-element torque converter is the by far most commonly used device to couple an automatic gearbox to an internal combustion engine. It is capable of decoupling and engaging the engine from the transmission in a fully automated and smooth way. The ability to multiply torque at low speed ratios, such as when starting from a stand-still can increase the acceleration performance to a significant degree. Because the connection between the engine and the transmission is viscous the torque converter also acts as a damper, smoothing out vibrations and the uneven torque delivery from the engine.

2.1.3 The lock-up clutch

As previously stated there is always some degree of slip between impeller and turbine and this constant slip equals a power-loss. At stall and low speed ratios the advantage of torque amplification usually outweighs the drawback of power-loss, but as the Speed Ratio increases the torque amplification is lost, while the power-loss is persistent. This can be solved by the introduction

of a so-called *lock-up clutch*, often integrated in the turbine assembly. As the Speed Ratio gets close to 1, meaning that the turbine speed is close to the impeller speed, the friction disc lock-up clutch will engage and lock the turbine to the torque converter housing. This effectively locks the impeller and turbine together, thereby eliminating the slip and the associated losses. During this mode of operation the Speed Ratio as well as the Torque Ratio is 1.

2.1.4 Modern torque converter design

The introduction of the lock-up clutch in 1949 was the final addition that gave the automotive torque converter the functionality it maintains to this day [4], [6]. Modern engineering tools, such as computer simulation and computational fluid dynamics (CFD), modern manufacturing techniques and modern material technology have all contributed to increased performance, but the basic functionality remains the same.
Perhaps the biggest change in automotive torque converters in recent years lies in the overall shape. Compared to a mechanical clutch, commonly used with manual transmissions, the torque converter generally needs more space, especially in the axial direction. Because of increasing space constraints recent years have seen a development towards so-called *flat-torus* or *squashed-torus* designs, as depicted by the figure below.

(a) Full-torus profile **(b)** Flat-torus profile

Figure 2.5: Torus profiles.

One drawback with the flat-torus design compared to the full-torus design is that efficiency is typically lower [3]. Development of improved friction materials as well as sophisticated control strategies for the lock-up clutch can however compensate for this by enabling the lock-up clutch to operate over a wider range, thereby raising the overall efficiency of the torque converter.

2.2 Torque converter modelling

This section describes three methods of modelling the behaviour of a torque converter. The first method is based on measured steady-state characteristics of the torque converter and it is this type of model that is currently used for complete vehicle simulation at Volvo Cars. The second method is a dynamic model based on hardware design parameters of the converter desired to model. This model takes fluid dynamics inside the converter into account, something that is not included in the previously mentioned model. The third approach is a quasi-dynamic model that is a combination of the two previous. It uses the same measured steady-state characteristics as the first model but also compensates for fluid dynamics using simplified equations based on the second model.

2.2.1 Current steady-state based model

As previously stated, Volvo Cars uses an in-house developed simulation tool called VSIM for complete vehicle simulation. VSIM is based on MATLAB and Simulink and consists of different subsystems such as engine, transmission, suspension and wheels that are connected to represent the complete vehicle. Each subsystem is broken down into components, such as the torque converter and the gearbox in the transmission subsystem. The current VSIM torque converter component is built based on look-up tables which relate the steady-state Torque Ratio (TR) and Capacity Factor (CF) to the Speed Ratio (SR). The torque transferred by the impeller and the turbine is calculated based on the look-up tables and Equation 2.8 and 2.9 below. The transferred torque is then inertia compensated in accordance with Equation 2.10 and 2.11. An example of a steady-state look-up table is presented below and in Appendix C.

Table 2.1: Example of steady-state look-up table.
Coupling point reached at SR=0.85.

Speed Ratio [−]	**Torque Ratio** [−]	**Capacity Factor** $[Nm \cdot 10^{-3}/rpm^2]$
0.00	2.14	3.272
0.10	1.99	3.257
0.20	1.84	3.228
0.30	1.70	3.181
0.40	1.56	3.112
0.50	1.43	3.017
0.60	1.30	2.887
0.70	1.18	2.713
0.80	1.06	2.481
0.85	1.00	2.370
0.90	1.00	1.842
0.95	1.00	1.237
1.00	1.00	0.187

$$T_{transferred,\ pump} = CF(SR) \cdot \omega_p^2 \tag{2.8}$$

$$T_{transferred,\ turbine} = TR(SR) \cdot T_{transferred,\ pump} \tag{2.9}$$

$$T_p = T_{transferred,\ pump} + \dot{\omega}_p \cdot I_p \tag{2.10}$$

$$T_t = T_{transferred,\ turbine} - \dot{\omega}_t \cdot I_t \tag{2.11}$$

where

T_p = Pump torque, cumulative torque from engine $[Nm]$
T_t = Turbine torque, torque to transmission $[Nm]$
ω_p = Pump angular speed $[rpm]$
$\dot{\omega}_p$, $\dot{\omega}_t$ = Angular acceleration of pump and turbine $[rpm^2]$
I_p, I_t = Inertia of pump and turbine $[kg \cdot m^2]$

Given the pump and turbine speed as input the model outputs pump and turbine torque in accordance with Equation 2.8, 2.9, 2.10 and 2.11, as shown in Figure 2.6. The model does not take inertia or fluid dynamics inside the converter into account. VSIM is however able to compensate for the inertias outside the torque converter model, but fluid dynamics are still not considered. Because of this, VSIM simulations tend to overestimate the transferred torque, thereby overestimating vehicle acceleration. Additionally, this torque converter model is empiric since it is based on measurement data

in the look-up tables. The only parameters outside the look-up tables that can be changed are the inertias, which leaves little room for optimisation.

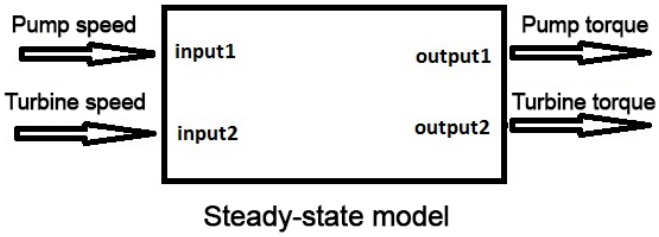

Figure 2.6: Torque converter model I/O in VSIM.
Inertias integrated outside the block in VSIM.

2.2.2 Dynamic model, Hrovat & Tobler

D. Hrovat and W. E. Tobler of the Ford Motor Company has derived equations for a state-space model capable of modelling transient performance of the torque converter [7]. The model is based on five assumptions:

1. The three-dimensional flow inside the converter is approximated by a flow along a meridional streamline.
2. The flow passage area is constant around the meridional streamline, which means that the axial fluid flow velocity is also constant.
3. Spacing between internal parts is not taken into account.
4. Blade thickness is not taken into account.
5. Thermal effects are not taken into account.

The model consists of four non-linear first-order equations. The first three equations, 2.12, 2.13 and 2.14, express the torque on the three elements (pump, turbine and stator). The fourth equation, 2.15, expresses the power-balance for the complete system. Compared to the current steady-state based model described in 2.2.1, the first term on the right hand side of Equation 2.12 and 2.13 corresponds to the transferred torque in Equation 2.8 and 2.9. The Hrovat & Tobler model does however not only consider inertia of the pump and turbine (first terms on the left hand side in Equation 2.12 and 2.13) but also fluid dynamics (second terms on the left hand side).

$$I_p\dot{\omega}_p+\rho S_p\dot{Q} = -\rho(\omega_p R_p^2+R_p\frac{Q}{A}\tan(\alpha_p)-\omega_s R_s^2-R_s\frac{Q}{A}\tan(\alpha_s))Q+T_p \quad (2.12)$$

$$I_t\dot{\omega}_t+\rho S_t\dot{Q} = -\rho(\omega_t R_t^2+R_t\frac{Q}{A}\tan(\alpha_t)-\omega_p R_p^2-R_p\frac{Q}{A}\tan(\alpha_p))Q+T_t \quad (2.13)$$

$$I_s\dot{\omega}_s+\rho S_s\dot{Q} = -\rho(\omega_s R_s^2+R_s\frac{Q}{A}\tan(\alpha_s)-\omega_t R_t^2-R_t\frac{Q}{A}\tan(\alpha_t))Q+T_s \quad (2.14)$$

$$\begin{aligned}&\rho(S_p\dot{\omega}_p + S_t\dot{\omega}_t + S_s\dot{\omega}_s) + \frac{\rho L_f}{A}\dot{Q} = \\ &\rho(R_p^2\omega_p^2 + R_t^2\omega_t^2 + R_s^2\omega_s^2 - R_s^2\omega_p\omega_s - R_p^2\omega_t\omega_p - R_t^2\omega_s\omega_t) \\ &+ \omega_p\frac{Q}{A}\rho(R_p\tan(\alpha_p) - R_s\tan(\alpha_s)) \\ &+ \omega_t\frac{Q}{A}\rho(R_t\tan(\alpha_t) - R_p\tan(\alpha_p)) \\ &+ \omega_s\frac{Q}{A}\rho(R_s\tan(\alpha_s) - R_t\tan(\alpha_t)) - P_{loss}\end{aligned} \quad (2.15)$$

Where (also see Table 2.2 below and Appendix B for details):

Q = Volume flow of the working fluid, $[m^3/s]$
A = Cross-sectional area perpendicular to the volume flow Q, assumed constant around the flow path, $[m^2]$
ρ = Density of the working fluid, $[kg/m^3]$
ω_p = Rotational angular speed of the pump, $[rad/s]$
ω_t = Rotational angular speed of the turbine, $[rad/s]$
ω_s = Rotational angular speed of the stator, $[rad/s]$
T_p = Pump torque, $[Nm]$
T_t = Turbine torque, $[Nm]$
T_s = Stator torque, $[Nm]$
S_p, S_t, S_s = Shape effect of pump, turbine and stator, defined as:

$$S_p = \int_0^{L_p} R_p \cdot \tan(\alpha_p)\ dl \quad (2.16)$$

$$S_t = \int_0^{L_t} R_t \cdot \tan(\alpha_t)\ dl \quad (2.17)$$

$$S_s = \int_0^{L_s} R_s \cdot \tan(\alpha_s)\ dl \quad (2.18)$$

L_p, L_t, L_s = length of the axial projection of the flow path contained within pump, turbine and stator.

The power loss function in Equation 2.15 is defined as:

$$\begin{aligned} P_{loss} &= \frac{\rho}{2} sgn(Q)(C_{sh,p}V_{sh,p}^2 + C_{sh,t}V_{sh,t}^2 + C_{sh,s}V_{sh,s}^2) \\ &+ \frac{\rho f}{2} sgn(Q)(V_{re,p}^2 + V_{re,t}^2 + V_{re,s}^2) \end{aligned} \tag{2.19}$$

Where $V_{sh,p}$, $V_{sh,t}$ and $V_{sh,s}$ are shock velocities defined as:

$$V_{sh,p} = R_s(\omega_s - \omega_p) + \frac{Q}{A}(tan(\alpha_s) - tan(\alpha_{pp})) \tag{2.20}$$

$$V_{sh,t} = R_p(\omega_p - \omega_t) + \frac{Q}{A}(tan(\alpha_p) - tan(\alpha_{tt})) \tag{2.21}$$

$$V_{sh,s} = R_t(\omega_t - \omega_s) + \frac{Q}{A}(tan(\alpha_t) - tan(\alpha_{ss})) \tag{2.22}$$

And $V_{re,p}$, $V_{re,t}$ and $V_{re,s}$ are fluid velocities relative to the blades defined as:

$$V_{re,p} = \frac{Q}{A} \cdot i_{r,p} + \frac{Q}{A} \cdot \tan(\alpha_p) \cdot i_{\phi,p} \tag{2.23}$$

$$V_{re,t} = \frac{Q}{A} \cdot i_{r,t} + \frac{Q}{A} \cdot \tan(\alpha_t) \cdot i_{\phi,t} \tag{2.24}$$

$$V_{re,s} = \frac{Q}{A} \cdot i_{r,s} + \frac{Q}{A} \cdot \tan(\alpha_s) \cdot i_{\phi,s} \tag{2.25}$$

Where i_r and i_ϕ are unit vectors in polar coordinates in the radial direction and tangential direction of the converter's central axis of rotation.

The other parameters are input parameters that needs to be measured, estimated or calculated. The parameters are shown in Table 2.2 below. An illustration of the geometrical parameters can be found in Appendix B.

Table 2.2: Input parameters.

I_p	Pump inertia	$[kg \cdot m^2]$
I_t	Turbine inertia	$[kg \cdot m^2]$
I_s	Stator inertia	$[kg \cdot m^2]$
ρ	Fluid density	$[kg/m^3]$
A	Flow area	$[m^2]$
R_p	Pump exit radius	$[m]$
R_t	Turbine exit radius	$[m]$
R_s	Stator exit radius	$[m]$
L_f	Equivalent fluid length	$[m]$
α_p	Pump exit angle	$[°]$
α_t	Turbine exit angle	$[°]$
α_s	Stator exit angle	$[°]$
α_{pp}	Pump inlet angle	$[°]$
α_{tt}	Turbine inlet angle	$[°]$
α_{ss}	Stator inlet angle	$[°]$
$C_{sh,p}$	Pump shock loss coefficient	[-]
$C_{sh,t}$	Turbine shock loss coefficient	[-]
$C_{sh,s}$	Stator shock loss coefficient	[-]
f	Friction loss coefficient	[-]

With the parameters in Table 2.2 known there are 7 unknown variables (speed of pump, turbine and stator; torque of pump, turbine and stator; fluid volume flow) in the state-space system. According to the torque converter operation principle described in 2.1.2 the stator operates in two different modes: locked or free-wheeling. When the stator is locked its rotational speed, ω_s, is 0 and when the stator is free-wheeling the stator torque, T_s, is 0. By dividing the model into these two cases the number of unknown variables can be reduced to 6. Lastly, by using two of the variables as input, only 4 unknowns remain and by using them as state variables the system of equations can be solved. For this particular implementation of the differential algebraic equation (DAE) system the input/output variables are pump torque, pump speed, turbine torque and turbine speed.
The state variables with locked stator: Q, T_p, T_t, T_s, ω_p, ω_t.
The state variables with free-wheeling stator: Q, T_p, T_t, ω_p, ω_t, ω_s.

With the approach used in VSIM, pump torque and turbine speed are inputs, which makes pump speed and turbine torque outputs, which is depicted in Figure 2.7.

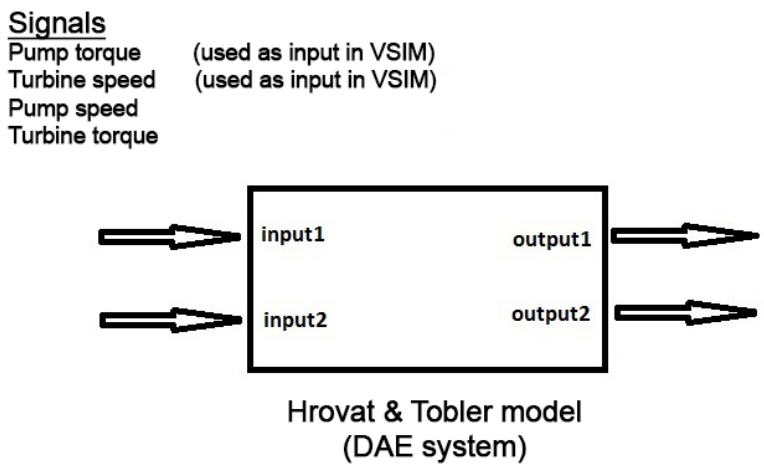

Figure 2.7: Hrovat & Tobler model I/O in VSIM.
Inertias integrated inside the block.

As previously stated this thesis only aims to examine transient characteristics, such as vehicle take-off. Because of this the coupling phase and freewheeling stator operation is ignored and ω_s is always treated as 0 in the model.

2.2.3 Dynamic model, Drenth

The two modelling approaches previously described are of very varying complexity. The look-up table based model relies on performance measurements and the inertias of the pump and turbine are the only parameters that can be changed. This means that computational demands are very low, which makes it fast. As previously stated it is however not suitable for modelling fast transient responses. By comparison, the Hrovat & Tobler model consists of four state-space equations which makes it capable of capturing transient dynamics, although calculation demands are much higher. Moreover, many parameters, some of which are difficult to measure or estimate, are required. As a compromise, Edo Drenth of Modelon AB has developed a Dymola model by combining the steady-state look-up tables with simplified equations from the Hrovat & Tobler model [10]. Essentially, these equations have the same states as the states in the Hrovat & Tobler model and the look-up tables are the same tables as used in the original VSIM torque converter model. The model was built in Dymola and implemented into VSIM with FMU-ME.
The Drenth model is not published and due to confidentiality a detailed description of the model can therefore not be presented in this report.

3
Verification

This section covers the verification of the different models. Three different methods were used: verification by comparison to manufacturer steady-state data, verification by comparison to driveline measurements in test rig and verification by comparison to in-vehicle measurements.

3.1 Model setup

Two torque converters with different stiffness were selected for verification. Both are used with the Aisin AW AWF8F gearboxes, denoted the F22-series at Volvo Cars.
To implement the Hrovat & Tobler model, the angles and radii listed in Table 2.2 were measured on cut open converters. Other parameters, such as flow area and flow path lengths could then be calculated. Lastly the parameters than could not be measured, such as loss coefficients, were obtained by using optimisation software to match simulation results to performance measurements by the manufacturer. These performance measurements are also what makes up the look-up tables used for the steady-state and Drenth model. The tables used in this thesis were supplied by the manufacturer, but could also be measured. An example of a steady-state look-up table can be found in Appendix C.
The three different torque converter models were implemented in two different environments as described below.

3.1.1 Mode 1: VSIM environment

In this mode the models were implemented in VSIM (replacing the steady-state based model described in Section 2.2.1) and complete vehicle simulations were performed. As previously mentioned VSIM is based on Matlab/Simulink while the Drenth model was written in Modelica. To implement the Drenth model into the VSIM environment, a Functional Mock-up Interface (FMI) was used as a block in the transmission subsystem in VSIM.

This enabled the Drenth model to be run directly in the complete vehicle simulations. For simplicity of integration into VSIM, the Hrovat & Tobler model was built in Simulink and could therefore be implemented in VSIM directly.
When implemented in VSIM, turbine torque and pump speed are outputs of the torque converter. Pump torque from the engine side is fed into the model as one of the inputs. Turbine speed is calculated based on turbine torque and vehicle data such as weight, velocity and acceleration and then used as the other input signal, as shown in Figure 3.1.

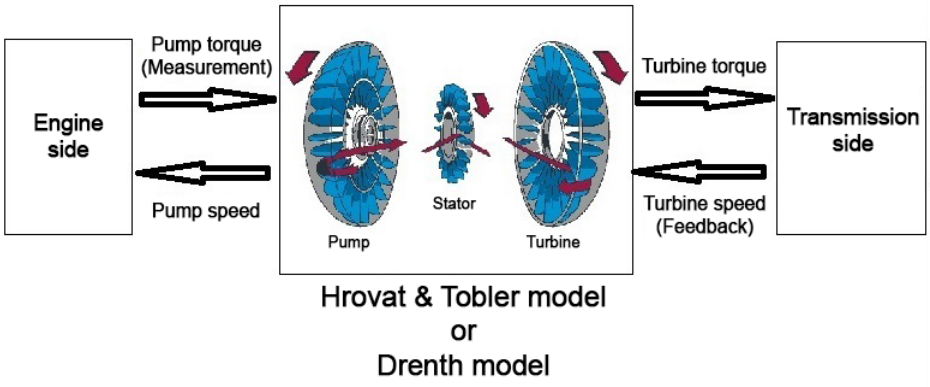

Figure 3.1: Mode 1, torque converter model in VSIM.

3.1.2 Mode 2: Isolated environment

In the VSIM model, turbine speed is calculated based on turbine torque and vehicle data. The turbine speed is then fed back to the torque converter model and used to calculate turbine torque at the next time step. This entails that possible errors will be passed on to the next time step, thereby causing an increasing error. To remove this influence, the torque converter can be implemented in an isolated environment, which only models the torque converter. This also removes errors that may be present in other subsystems in VSIM. In this environment the inputs are still the pump speed and turbine torque, but instead of simulated values from VSIM, data from in-vehicle measurements are used.

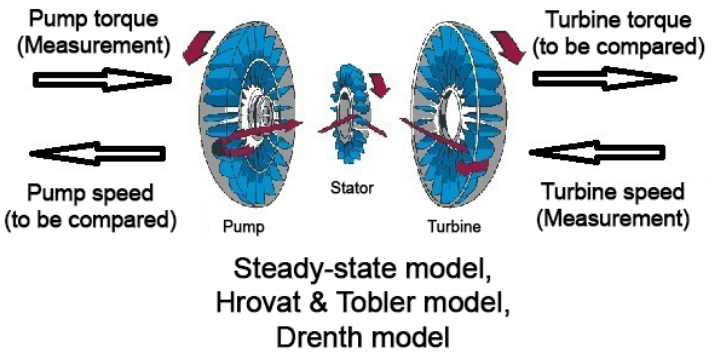

Figure 3.2: Mode 2, isolated torque converter model.

Since simulation by mode 1 is a full vehicle simulation, output data can be for instance vehicle acceleration and vehicle speed. As previously mentioned the implementation used in this case may however be sensitive to feedback errors. Because of the high complexity of VSIM and the high number of submodels it can also be difficult to analyse the results, since there are many sources of errors. Simulation by mode 2 is less complex with less sources of error and the torque converter isolated, which removes influence from other models. Mode 2 can however only give output data on component level, typically pump speed and turbine torque.

3.2 Steady-state characteristics

The first step of the verification process was to match the steady-state performance of the simulation models to measurement data. For the Hrovat & Tobler model some parameters, such as loss coefficients, needs to be calculated and verified by iteration against measurements.

3.2.1 Verification to manufacturer data

The method used for both the Hrovat & Tobler and the Drenth model was to input a fixed impeller speed and then vary the turbine speed to cover speed ratios from 0 to 1. The models were run until steady-state was reached and the Torque Ratio and Capacity Factor was calculated and compared to values supplied by the manufacturer. The results for one of the converters are presented in Figure 3.3 and 3.4. Note that the y-axis does not start at 0 and

that specific values are not presented due to confidentiality. Also, the results for the Hrovat & Tobler model are cut off at SR=0.85 since the implemented version of the model is not valid above the coupling point.

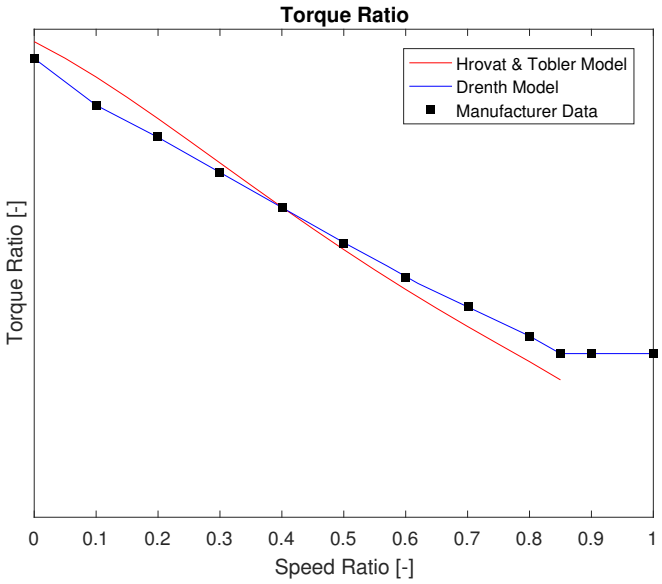

Figure 3.3: Comparison of Torque Ratio.

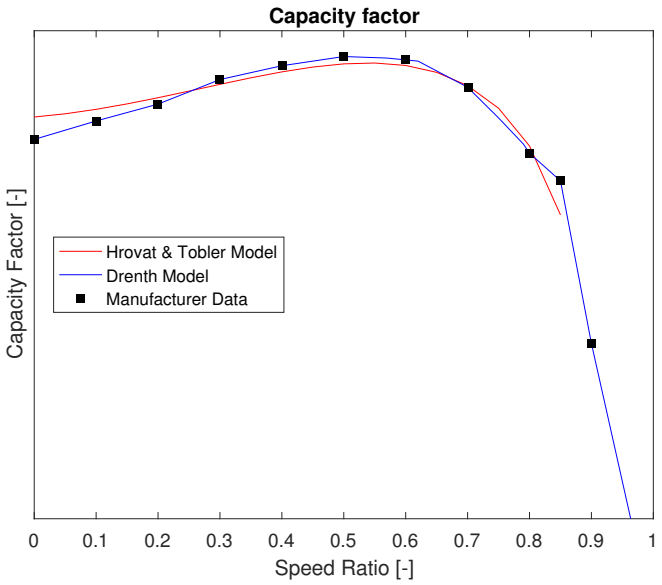

Figure 3.4: Comparison of Capacity Factor.

As previously mentioned, the steady-state look-up table used in the Drenth model is based on the performance measurements supplied by the manufacturer. For this reason the steady-state performance of the Drenth model is identical to input data, as seen in Figure 3.3 and 3.4.
Under steady-state conditions, the left-hand sides of Equation 2.12, 2.13, 2.14 and 2.15 are zero and the Hrovat & Tobler model performs according to the right-hand sides of the equations. This means that even under steady-state conditions, the model performance is based on geometrical parameters measured on a physical converter. The model is however based on the mean fluid flow path inside the converter, which might not correlate perfectly with the actual blade angles and element radii. Because of this, and the fact that some parameters such as friction and loss coefficients can not be measured, the parameters needs to be fine-tuned to make the model match manufacturer performance data.
During this parameter matching it was however found that the model was unable to match the manufacturers data while maintaining the blade angles within reasonable values (with regard to measured values). This is further elaborated in Section 4.3.2.

3.2.2 Comparison with steady-state based model

The Hrovat & Tobler model and the Drenth model were compared with the original steady-state based model used in VSIM. The three models were implemented in VSIM separately according to Mode 1 and a full vehicle simulation was run. The test setup simulates a full-throttle acceleration from stand-still in a Volvo S90 with an F22-gearbox and the stiffer torque converter.
The vehicle is put in first gear and held stationary for five seconds by applying the brakes. During this period the torque converter should perform identically, or very close to, steady-state performance. After five seconds the brake is released and the throttle fully depressed. During the initial acceleration the conditions inside the converter will be highly transient and the performance should be significantly different from the steady-state measurements. After a short period the transient effects will however lessen and the performance should be closer to steady-state again.
The full simulation is run from 0 to 100 km/h as this is a pre-defined driving cycle in VSIM, but since this thesis only focuses on the initial phase of the acceleration and the implementation of the Hrovat & Tobler model is only valid up until the coupling point, only the first seconds of the acceleration is analysed. Torque Ratio and Speed Ratio can be seen in Figure 3.5 and corresponding vehicle acceleration is shown in Figure 3.6.

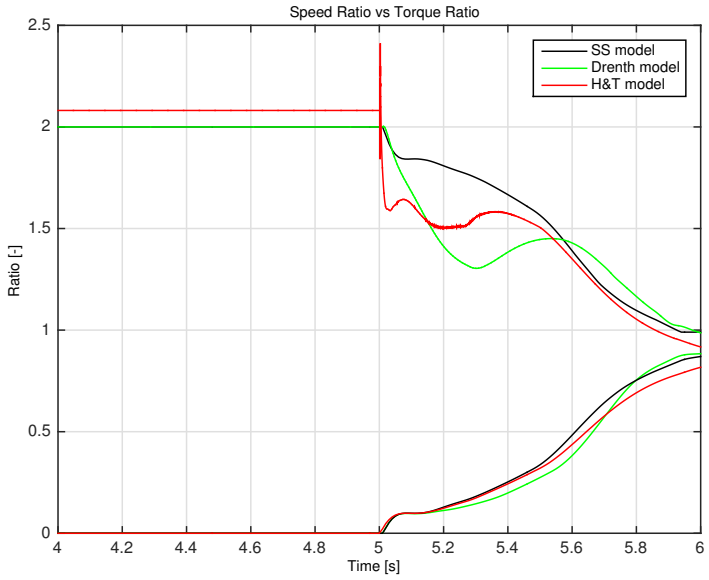

Figure 3.5: Comparison of the three models; upper lines are Torque Ratio, lower lines are Speed Ratio.

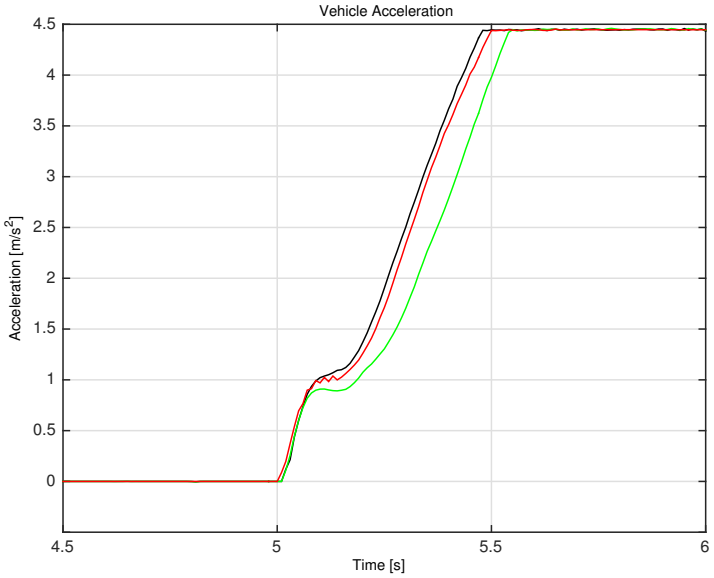

Figure 3.6: Comparison of the three models; vehicle acceleration. Legend as in Figure 3.5.

As Figure 3.5 shows, the three models show quite different behaviour during the initial acceleration phase, as was expected. The original VSIM model and the Drenth model are based on the same steady-state look-up tables and therefore show identical performance during the stall phase (up until the 5 second mark). The Hrovat & Tobler model slightly over-estimates the Torque Ratio at stall, as was previously shown in Figure 3.3 and discussed in Section 3.2.1. It can be found that the Torque Ratio during the initial acceleration is significantly lower for the two dynamic models, which is expected since the models also take fluid dynamics into account. After the initial drop the dynamic models begin to conform with the steady-state based model and after approximately 0.6 seconds of acceleration the three models show similar performance. At this point the dynamic terms in the Hrovat & Tobler and Drenth models are small, indicating that fluid dynamics only have a slight influence and that the torque converter operates close to steady-state performance. As a result of the difference in Torque Ratio, the models also give different vehicle acceleration, as can be seen in Figure 3.6. The initial acceleration from the two dynamic models is lower than the steady-state model since the torque transferred from pump to turbine is lower.
This comparison shows that the two dynamic models are capable of capturing realistic steady-state behaviour. Their behaviour during the transient phase differs significantly from steady-state performance, which was expected and will be analysed in the following sections.

3.3 Verification of estimated engine torque

The input torque to the torque converter is the net output torque of the engine, often denoted crank torque. This is usually measured by connecting the engine directly to a dynamometer, by measuring the output torque from the gearbox (drive shaft torque) in a drivetrain rig or by running the complete vehicle on a so-called rolling road dynamometer, where the drive-wheel torque is measured. In the two latter cases the crank torque must then be backwards-calculated based on gear ratio, transmission losses etcetera. One drawback with this kind of testing is that in order to simulate real-world driving, the dynamometer needs to simulate these real-world conditions, e.g. apply resistance in accordance with the desired drive cycle, something that must be measured and calibrated.
Another common way to measure torque during real-world driving is to equip the vehicle with torque measuring drive shafts. These drive shafts are equipped with strain gauges and by measuring the deformation (twisting) of the drive shafts the transmitted torque can be calculated.

All of the techniques described above require varying degrees of preparation, equipment, mechanical work and calibration and are therefore both time consuming and expensive. The engine torque is however also estimated by the Engine Control Module (ECM) based on operating parameters such as intake air flow and injected fuel mass. As part of the thesis this estimated engine torque will be compared against verified dynamometer measurements to evaluate the accuracy of the prediction. If the error of the estimated torque is within reasonable limits there will be a great potential for saving resources in future testing, since the engine torque could then be logged directly in the vehicle.
The data used for this analysis is so-called "Time-To-Torque" (TTT) data, which is a common way to measure engine load response. The engine is run at a fixed speed and zero brake torque. Full throttle is then applied and the torque response measured. The plot below shows an example of load response curves for a Diesel engine at speeds between 1.000 and 4.250 rpm.

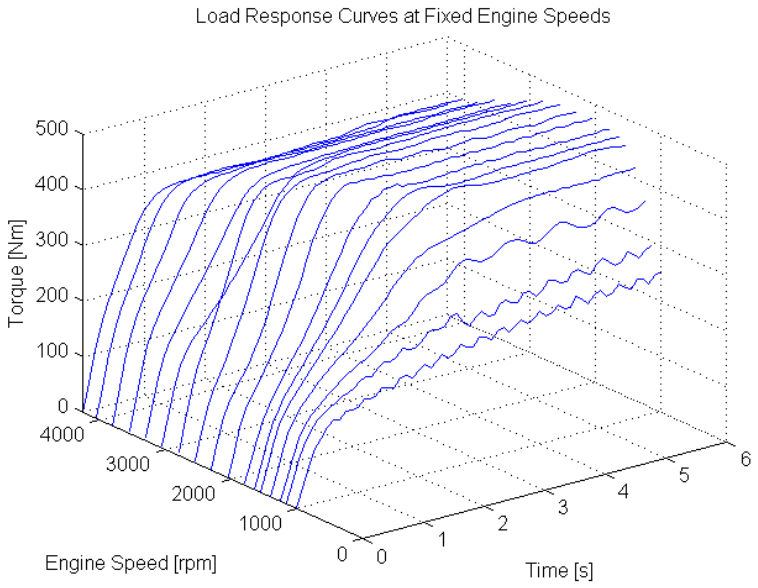

Figure 3.7: Load response curves at fixed engine speeds.

By comparing the estimated engine torque to the measured dynamometer torque, the error in torque estimation can be evaluated. The analysis was made based on data from previous testing performed at Volvo Cars but it was found that the sampling frequency of the estimated torque was too low to be used in this analysis. An example of a measurement that illustrates this problem is shown below.

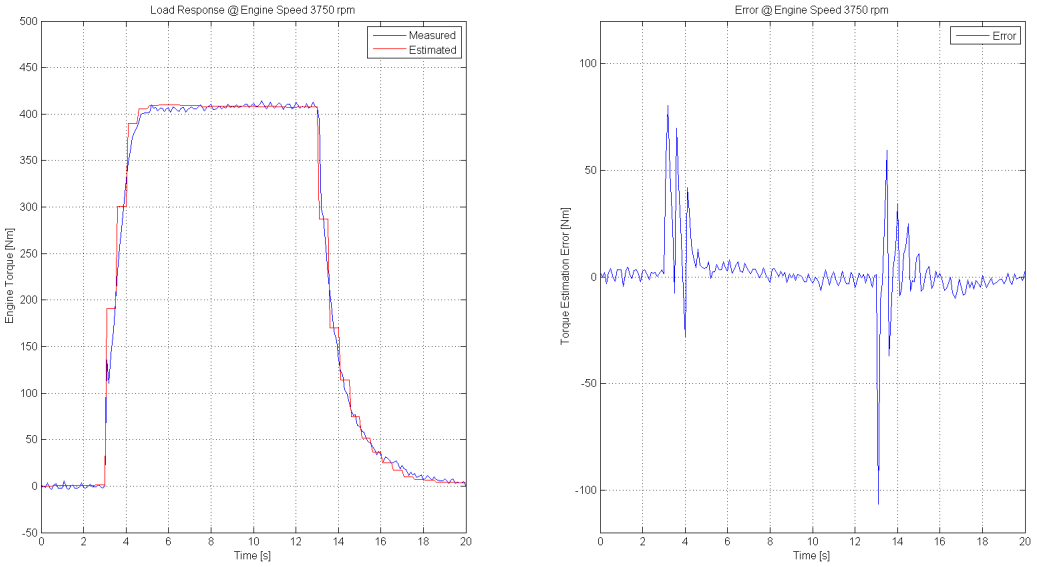

Figure 3.8: Measured and estimated load response and estimation error at 3750 rpm.

As can be seen, the low sampling frequency of the estimated engine torque signal causes large steps during fast transients. Because of this the instantaneous error between the signals is substantial.
It should also be noted that this approach is not entirely accurate for describing the torque build-up during a vehicle launch, since the engine speed will not be fixed.

3.4 Transient characteristics: By rig test

When the parameters necessary for the Hrovat & Tobler model are calculated and the steady-state performance of both models is verified, the models can be tested with transient, non-simulated input data. The first approach to perform this verification is to use data from a drivetrain rig, as depicted below.

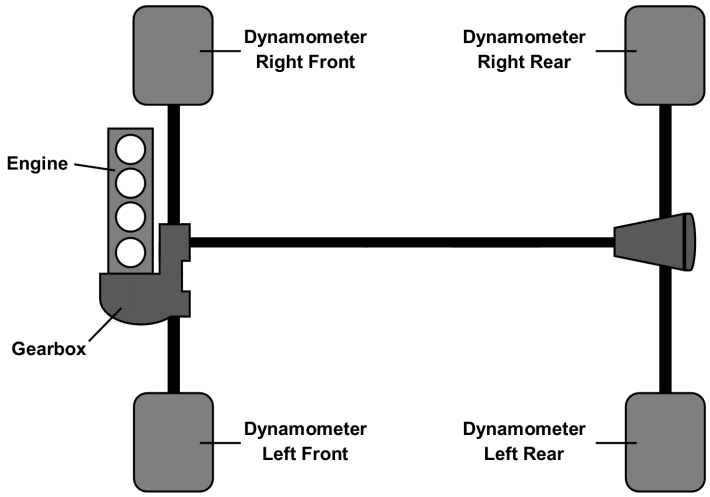

Figure 3.9: Schematic of drivetrain rig.

3.4.1 Test setup

For the subject of this thesis it would be desirable to run full throttle accelerations in the test rig, but because of on-going scheduled tests this was not possible within the time frame. Because of this, the test data used is from the US06 driving cycle used for emission measurements. The cycle was selected since it contains several accelerations from stand-still, although not at full throttle. The vehicle speed during the US06 driving cycle can be seen in Figure 3.10. The take-off marked in red in the figure is selected for the analysis.

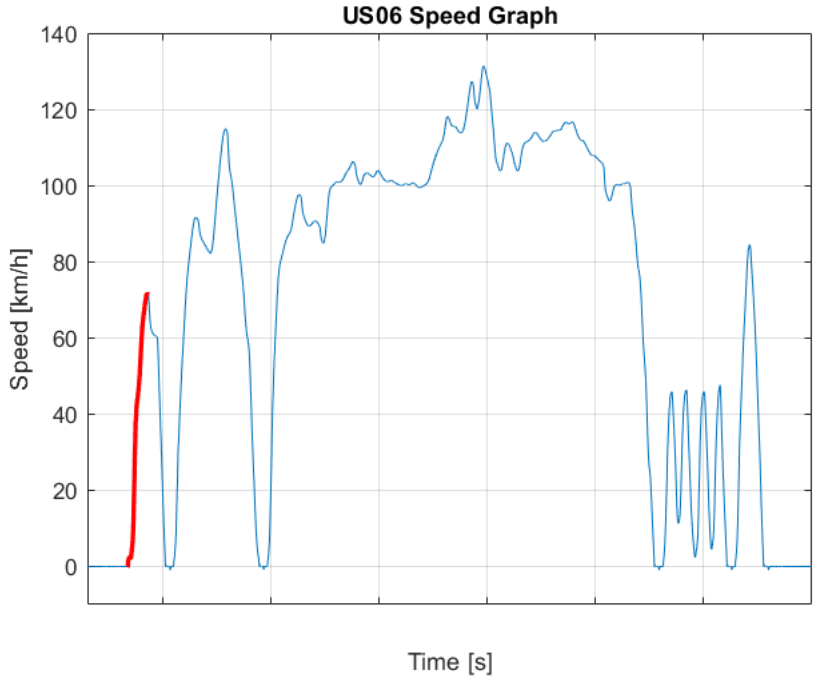

Figure 3.10: Vehicle speed in US06 driving cycle.

The powertrain used in the tests was a VEP4 HP engine coupled to an F22 AWD transmission with the stiffer torque converter.

Captured signals:

- Pump speed, ω_p. Calculated from engine speed.
- Pump torque, T_p. Based on estimated engine torque as described in Section 3.3 below.
- Turbine speed, ω_t. Calculated from dynamometer speed.
- Turbine torque, T_t. Calculated from dynamometer torque, compensated for inertia and transmission losses.

3.4.2 Results

The acceleration marked with red in Figure 3.10 was selected for analysis, as previously stated. Only the initial part of the acceleration was analysed, since the implementation of the Hrovat & Tobler model is only valid for locked stator and open lock-up. The comparison between simulation and test is presented below.

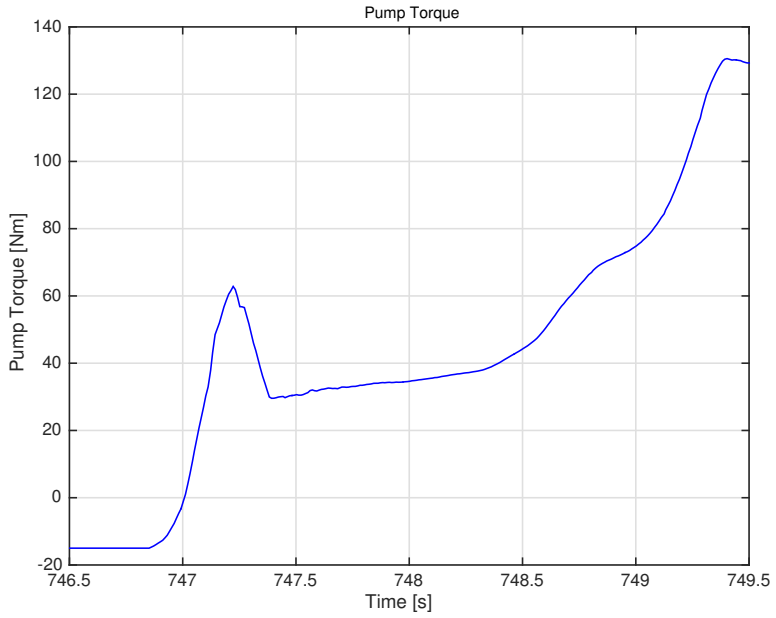

Figure 3.11: Pump torque signal from test rig (used as input).

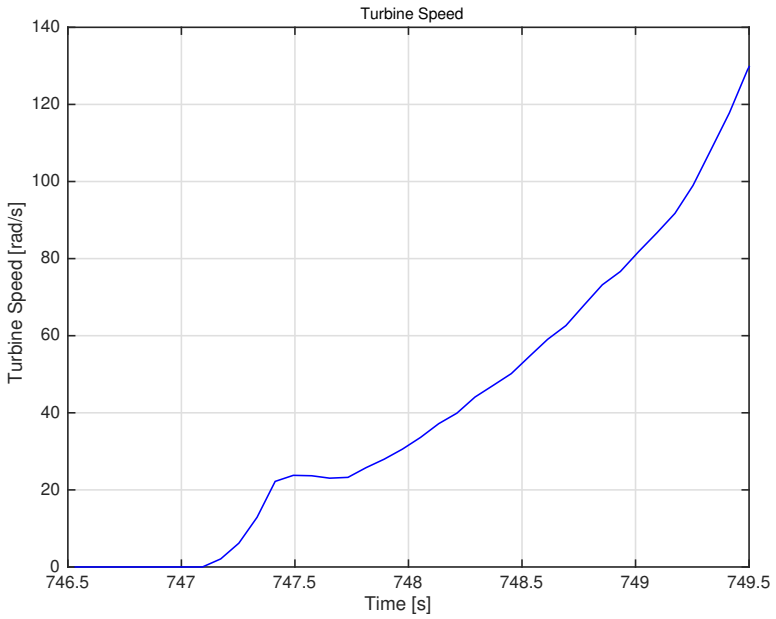

Figure 3.12: Turbine speed signal from test rig (used as input).

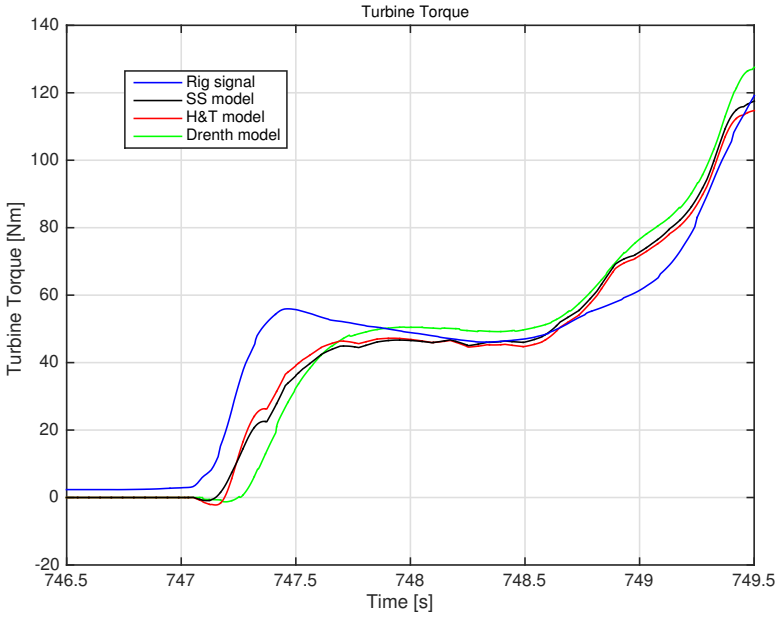

Figure 3.13: Comparison of turbine torque (output).

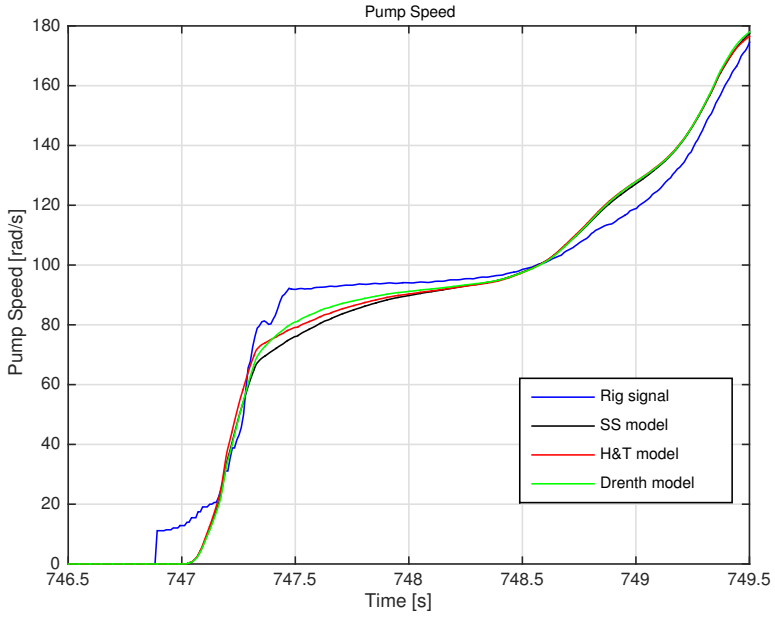

Figure 3.14: Comparison of pump speed (output).

As can be seen, the turbine speed is 0 up until approximately 747 seconds, indicating that the vehicle is stationary. It can also be noted that the pump speed is 0 at the start of the period, since the test was run with the start-stop function activated. Slightly before 747 seconds the engine is cranked, at the 747 second mark the torque output is positive and the vehicle starts to accelerate.
From the above figures it can be seen that simulated turbine torque and pump speed from the steady-state based model and the two dynamic models are similar to the rig data. The turbine torque from the dynamic models is slightly different compared to the steady-state model since fluid dynamics influence both the pump transferred torque and the turbine transferred torque. The difference is however small since the acceleration is quite slow and hence the converter works close to steady-state performance (influence of fluid dynamics is small).
At approximately 749.5 seconds the converter reaches the coupling point, and since this is not considered in the implementation of the Hrovat & Tobler model, the data after this point is not analysed.

3.5 Transient characteristics: By in-vehicle measurements

To verify the model performance in in-vehicle simulation, both the Hrovat & Tobler model and the Drenth model are implemented by the two different modes previously described. The simulated results are then compared with results from complete vehicle measurements.

3.5.1 Test setup

Vehicle: Volvo S90 AWD, VEP MP engine, F22 gearbox.
Driving cycle: Acceleration from standstill. Brake pedal is held for 5 seconds and then released at the same times as full throttle is applied (flip-flop launch).
Signals captured: Vehicle acceleration, engine speed, gearbox input speed, estimated engine crank shaft torque and estimated turbine torque.

3.5.2 Results

In both the Hrovat & Tobler model and the Drenth model, the effect of inertia and fluid dynamics during transients can be regarded as torques.

By modelling them as torque losses during the torque transfer the following equations can be used to express the torque flow shown in Figure 3.15 below:

$$T_{inertia,p} + T_{fluid,p} + T_{transfer,p} = T_p \tag{3.1}$$

$$T_{inertia,t} + T_{fluid,t} + T_t = T_{transfer,t} \tag{3.2}$$

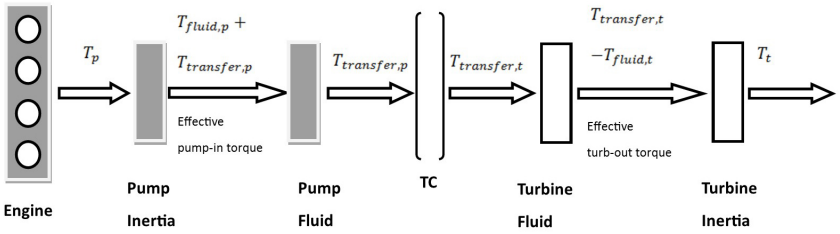

Figure 3.15: Torque flow sketch.

The fluid torque is the most significant difference between the two dynamic models and the steady-state based. This dynamic torque influences the torque transferred from pump inertia to turbine inertia. The torque at these two points can be seen as the effective pump input torque and effective turbine output torque. In the measurement data, the torque at these two positions can be calculated by Equation 3.3 and 3.4.

$$T_{effective,in} = T_{measurement,eng} - I_p \cdot \dot{\omega_p} \tag{3.3}$$

$$T_{effective,out} = T_{measurement,GB} + I_t \cdot \dot{\omega_t} \tag{3.4}$$

where $T_{measurement,eng}$ is the estimated engine torque as described in 3.3, $T_{measurement,GB}$ is the torque transferred from converter to gearbox, which is calculated from vehicle speed, acceleration and mechanical losses in the transmission.

3.5.2.1 Isolated torque converter simulation

In this case the different torque converter models are implemented in Simulink separately, as shown in Figure 3.2. The input data to the models is estimated engine torque and measured turbine speed. Effective pump input torque and effective turbine output torque can be calculated according to Equation 3.3 and 3.4 based on the output from the simulation, as descried above. The comparison between measurement and simulation is presented below.

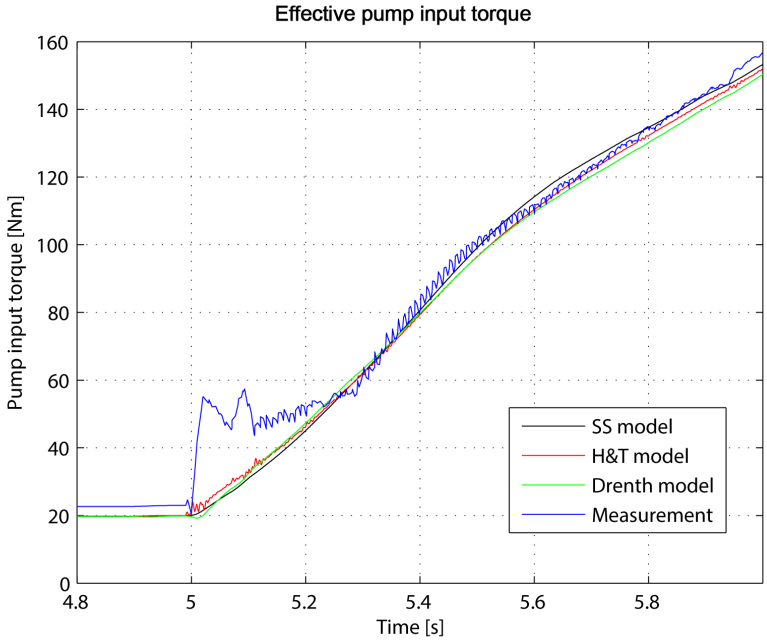

Figure 3.16: Comparison of effective pump input torque.

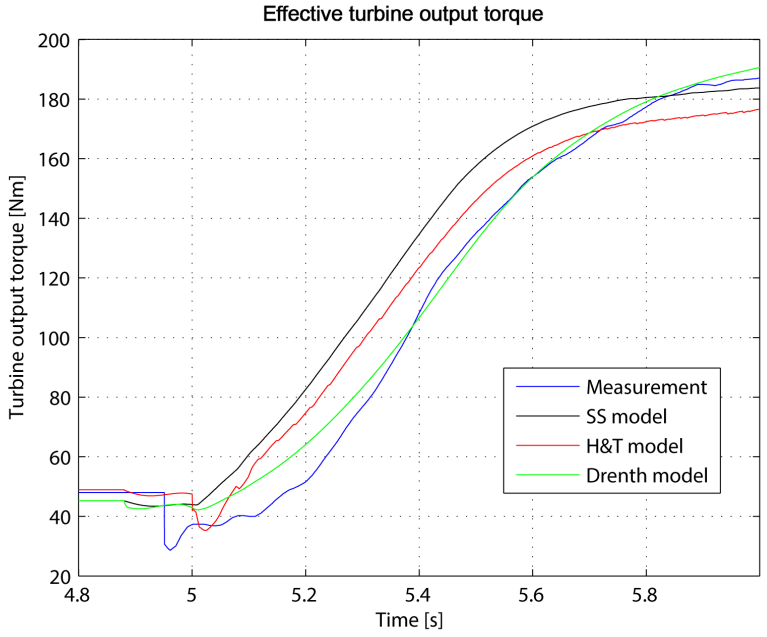

Figure 3.17: Comparison of effective turbine output torque.

As can be seen from Figure 3.16, the effective pump input torque is similar among the models, except for a clear discrepancy between all three models and the measured data during the first 0.2 seconds. The input torque is calculated from the estimated engine crank torque, which is uniformed in measurement and simulation. Possible reasons for the discrepancy during the first 0.2 s will be examined in the next chapter.
The effective turbine output torque, presented in Figure 3.17 shows a clear difference between the three models and it can be noted that the two dynamic models perform closer to the measurement than the steady-state based model. As illustrated on the pump side in Figure 3.15, the pump fluid torque is subtracted from the engine torque, to give the transferred pump torque. This causes the transferred pump torque in the dynamic models to be lower than in the steady-state based model, which in turn causes lower turbine torque. On the turbine side, the turbine fluid torque is also subtracted from the transferred turbine torque to calculate the effective turbine output torque. Therefore transferred pump torque, transferred turbine torque and effective turbine output torque are all lower in the dynamic models, and show a higher similarity with the measurements.

3.5.2.2 Complete vehicle simulation in VSIM

The simulation was then extended to cover a complete vehicle in VSIM. As mentioned previously, results from this mode of simulation are likely not as accurate as results from isolated component simulation. Since the complete vehicle is simulated it is however possible to output data on vehicle level, such as acceleration.
In this case the different torque converter models were implemented into VSIM as described in Section 3.1.1. It should be noted that there will be discrepancies between engine output torque captured in in-vehicle tests and engine output torque simulated by the engine model in VSIM. To reduce the influence from this difference the engine subsystem in VSIM was replaced by output signals logged during the in-vehicle tests.
The comparison between measurement and simulation is presented below.

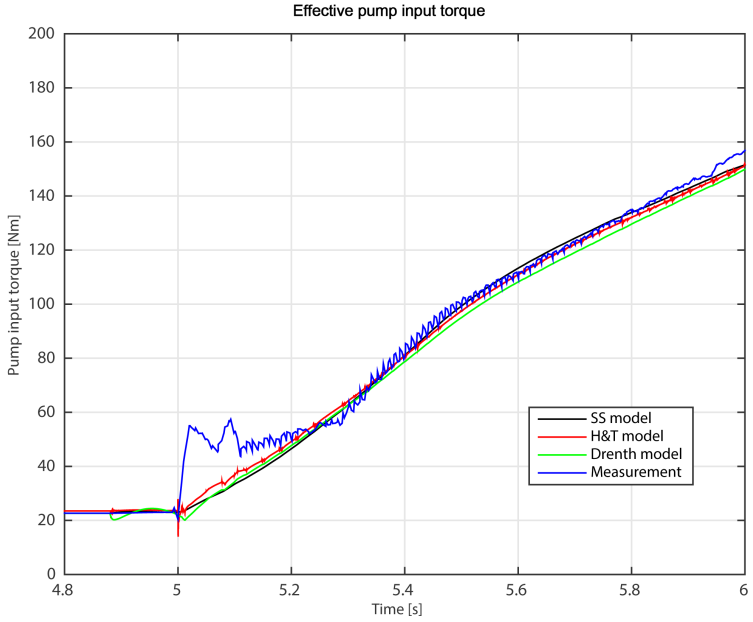

Figure 3.18: Comparison of effective pump input torque.

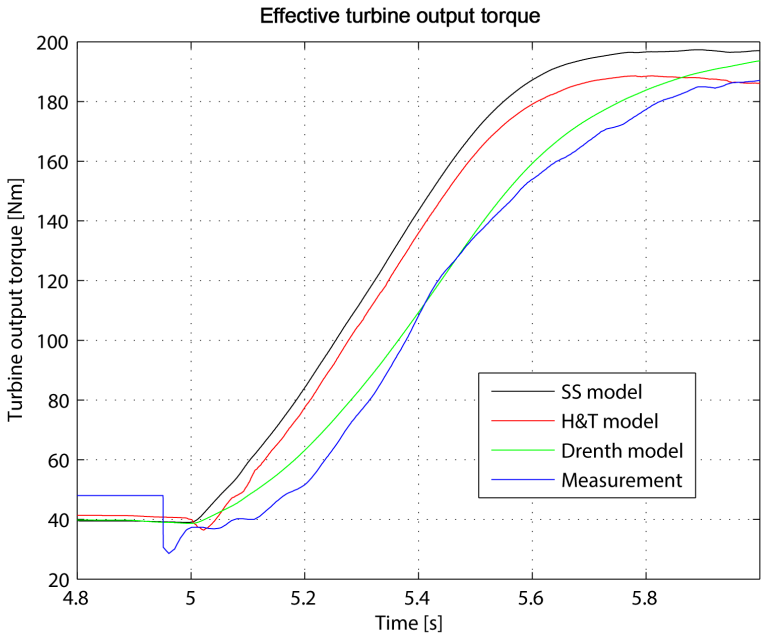

Figure 3.19: Comparison of effective turbine output torque.

Similar to the results obtained in the isolated component simulations, effective turbine output torque by the dynamic models is lower than the results from the steady-state based model and show a higher resemblance with the measurements. This has a direct influence on the vehicle acceleration as shown below.

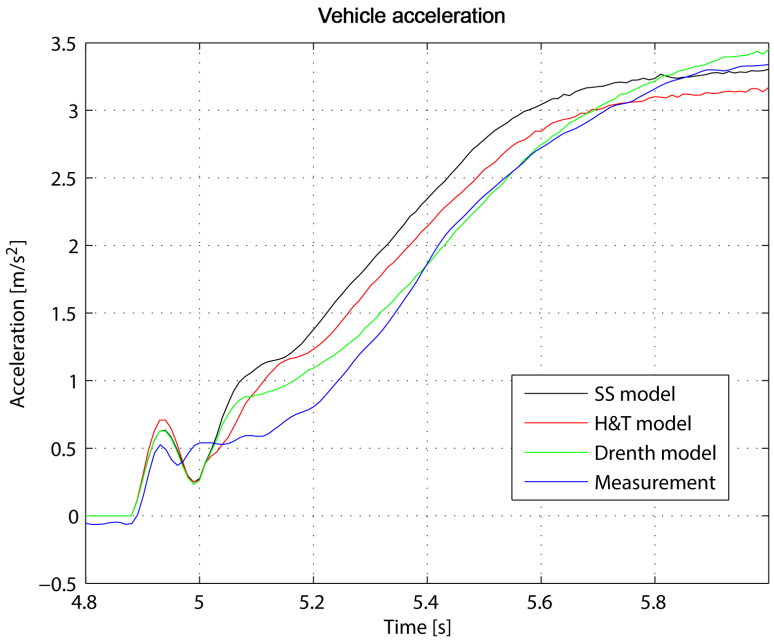

Figure 3.20: Comparison of vehicle acceleration.

The vehicle acceleration was used to verify the models during complete vehicle simulation. As can be seen from Figure 3.20, the simulated acceleration from the Hrovat & Tobler model and the Drenth model are both lower than the acceleration from the steady-state model and show higher resemblance to the measured data.
Note:

1. The converter reaches the coupling point at approximately 6 seconds, the results after this time are not analysed.
2. The Hrovat & Tobler model over-estimates the turbine torque and therefore also vehicle acceleration.
3. The Drenth model also over-estimates the turbine torque, but to a lesser degree and shows higher resemblance with the measurement data.
4. The error in effective pump input torque during the first 0.2 seconds is significant.

The last three points will be elaborated further in the next chapter.

4

Comparison and analysis

4.1 Optimisation

As described by Equation 3.1 and 3.2, the fluid dynamic terms are the main difference between the dynamic models and the steady-state based model. In the torque flow from pump to turbine, fluid dynamics in both components will cause losses in torque transfer. Apart from the inertias, the shape effect factors in Equation 2.12 and 2.13 have the largest influence on the effective torque amplification during transients. To analyse the influence from the shape effect factors, both dynamic models were run with different shape effect values. The analysis was performed both for the complete vehicle simulation in VSIM as well as the isolated converter.
The results are presented below. S_p and S_t are the shape effect factors for the pump and turbine, respectively.

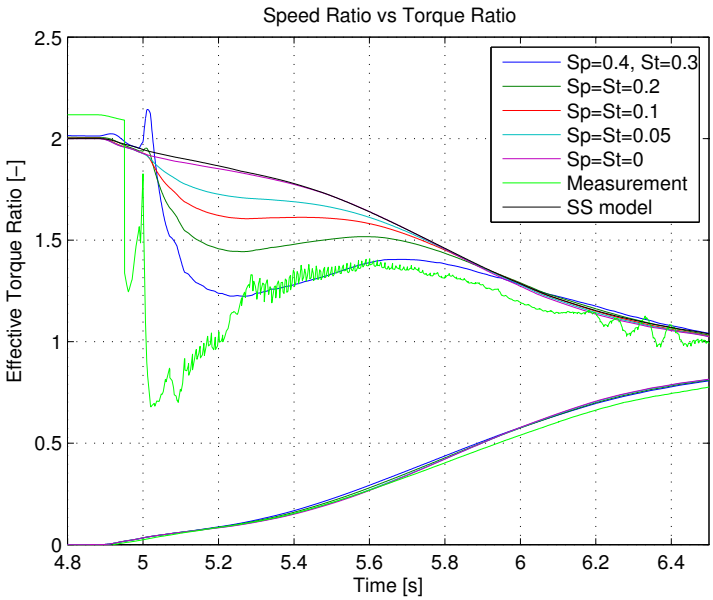

Figure 4.1: Influence of shape effect on effective Torque Ratio. Drenth model, isolated converter.

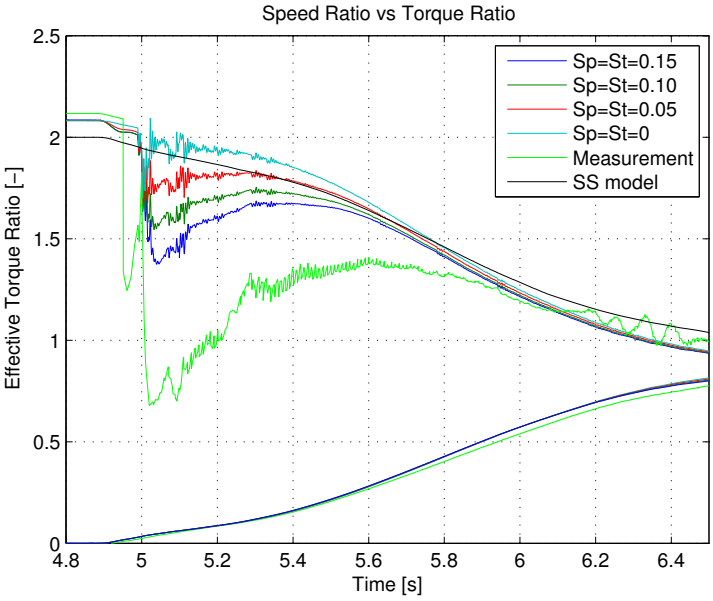

Figure 4.2: Influence of shape effect on effective Torque Ratio. Hrovat & Tobler model, isolated converter.

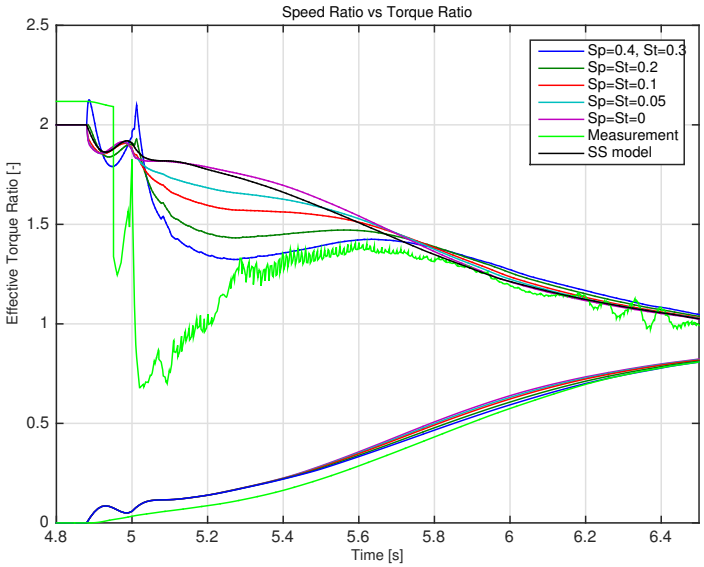

Figure 4.3: Influence of shape effect on effective Torque Ratio. Drenth model, VSIM.

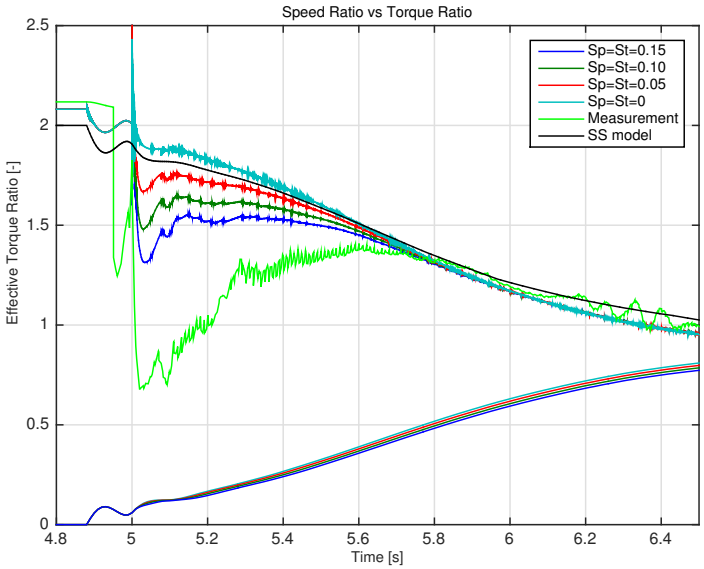

Figure 4.4: Influence of shape effect on effective Torque Ratio. Hrovat & Tobler model, VSIM.

As shown by the figures, a larger shape effect causes a more significant drop in effective Torque Ratio during transients. When the shape effect is 0, the dynamic models perform very close to the behaviour of the steady-state based model. A larger shape effect causes larger fluid dynamic torques which reduces the effective torque amplification and hence gives lower acceleration of the vehicle in the VSIM simulations. Results of vehicle acceleration from the VSIM simulations are presented below.

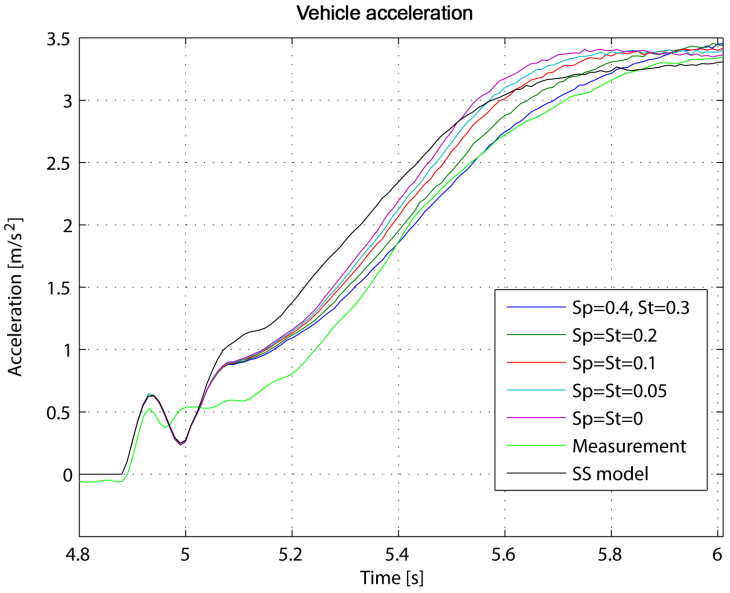

Figure 4.5: Shape effect influence on vehicle acceleration, Drenth model.

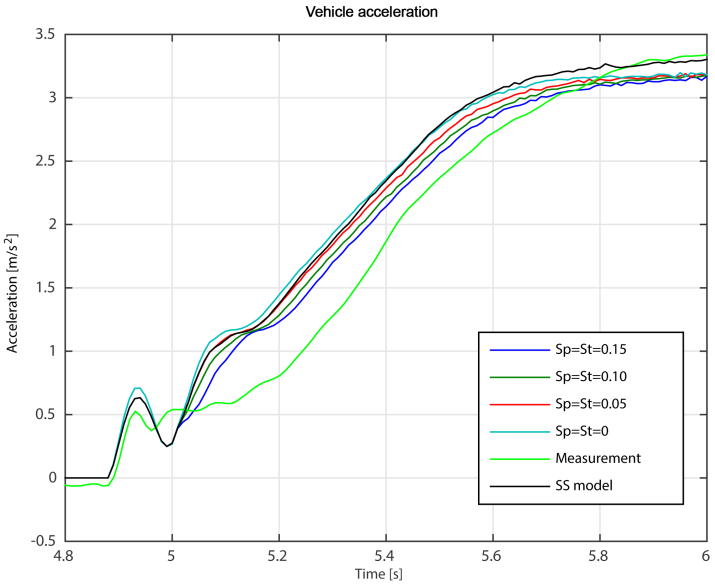

Figure 4.6: Shape effect influence on vehicle acceleration, Hrovat & Tobler model.

The shape effect parameters used in the Hrovat & Tobler model are calculated in accordance with equations 2.16 and 2.17 and hence are constants for a particular converter design. Since they are the only design parameters that influence the fluid dynamics in the torque equations (2.12 and 2.13), the approach used above was to increase the values of the shape effect factors to evaluate if the model was capable of matching the drop in the measurement data seen in Figures 4.2 and 4.4. In the Drenth model the shape effect factors are used as constants for curve-fitting and not calculated based on geometric parameters.
To make the results from the Hrovat & Tobler model match the measurements, a comparably large shape effect would be required, but when the shape effect factors gets to large the model will crash due to solver issues in Simulink. The model also contains several algebraic loops which require very small time steps with larger shape effect values, which makes the simulation time unreasonably long. Because of this the Hrovat & Tobler model could only be run with shape effect factors up to 0.15. The Drenth model was run with factors up to $S_p = 0.4$ and $S_t = 0.3$ since this provided the best match for the Torque Ratio curves.

4.1.1 Shape effect optimisation

According to the results presented above, it is desirable with small shape effect values, since this will improve torque transfer during transients and make the converter behave closer to the steady-state performance. Shape effect is a function of exit radii, exit angle and the length of the axial projection of the fluid flow line contained within the pump and turbine respectively.

$$S_p = \int_0^{L_p} R_p \cdot \tan(\alpha_p)\ dl \tag{4.1}$$

$$S_t = \int_0^{L_t} R_t \cdot \tan(\alpha_t)\ dl \tag{4.2}$$

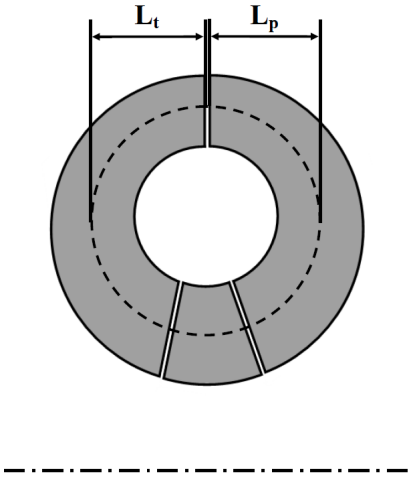

Figure 4.7: Axial projection of meridional streamline.

This suggests that a smaller diameter (smaller exit radii), axially thinner (shorter length of the axial projection) converter with less aggressive flow redirection (lower blade exit angles) would be beneficial in this context. Since radii and blade angles will also influence the steady-state characteristics, thus influencing the overall performance of the torque converter, the study presented in Section 4.1 focused only on the shape effect. No other parameters were changed, in order not to affect the steady-state characteristics. A smaller and thinner (more squashed) converter also has the potential to be lighter and will hold less fluid, both of which could lower the inertia, thereby improving response and effective torque transfer during transients. As previously stated the parameters can however have significant effects on other areas as well and hence further investigation would be needed when

designing the converter. The theoretical torque capacity of a converter can for instance be estimated by $\rho \cdot \omega_p^2 \cdot D^5$, where ρ is the density of the working media, ω_p is the pump speed and D is the converter outside diameter, which is roughly equal to the pump exit radius. Since the outside diameter is held to the power of 5, it should be clear that it has a very significant impact on torque capacity. Automotive torque converters are commonly about 230-300 millimetres in diameter, with axial projections of the impeller and turbine measuring approximately 30-50 mm. Impeller exit angles are commonly around 20° and rarely exceed 45°, while turbine exit angles are usually around 60° [6]. These values can be used to estimate reasonable values for the shape effect.

4.2 Comparison of the dynamic models

As previously mentioned, the Drenth model is built based on steady-state look-up tables and simplified equations from the Hrovat & Tobler model. It has however been shown that there are significant differences between the results from the two models. Some of the differences, drawbacks and strong points of the two models will be compared and discussed in the following parts.

4.2.1 Inaccuracy and drawbacks of the Hrovat & Tobler model

For steady-state simulations the main drawback of the Hrovat & Tobler model is the high number of geometrical parameters, which requires many measurements. Since the model is built based on that the fluid follows a single meridian streamline inside the converter, the actual blade angles in the converter may not give the desired results when implemented in the model. It is also known that the flow inside the converter will change significantly over the operating range, meaning that the actual exit and inlet angles as well as the exit and inlet radii between the different converter elements will not be constant [3]. This is however not taken into account by the model since the same geometric parameters are used over the entire operating range. This compromise will inevitably lead to inaccuracies, and this is likely also part of the reason that the model could not be perfectly matched to measured converter performance, as described in Section 3.2.1. The difference in both Torque Ratio and Capacity Factor seen in Figures 3.3 and 3.4 will also cause inaccuracies during transient simulations.
Furthermore, the model assumes that the flow path inside the converter is

perfectly circular. When the model was derived in the mid 1980's this was a reasonable approach, but as discussed in Section 2.1.4, modern torque converters tend to be of the squashed-torus design. As described in Section 4.1 and shown in Figures 4.2 and 4.4 the Hrovat & Tobler model was not able to capture the drop in Torque Ratio as seen in the measurements.
Data presented by Brad Pohl (2003) suggests that full-torus converters are less sensitive to transients [8]. A squashed-torus converter will show a more significant drop in Torque Ratio during transients and this drop will increase the more squashed the converter is and the faster the transient is [8]. Based on these findings, the Hrovat & Tobler model may not be suitable for simulation of highly squashed converters.
The model may also not be as suitable for evaluation of design concepts as first anticipated, because of the difference between the mean flow path and the actual converter hardware parameters. Though the model seems suitable for analysing trends and to get a deeper understanding of torque converter design, it is likely not accurate enough for fine-tuning, but can be suitable for analysing starting points for further evaluation.

4.2.2 Inaccuracy and drawbacks of the Drenth model

To reduce the complex calculations of the Hrovat & Tobler model, steady-state terms and dynamic terms are separately calculated in the Drenth model. The steady-state term is read from the look-up table and the dynamic term is calculated according to equations presented in Section 2.2.3. This causes an inaccuracy because the relation between steady-state components and dynamic components is ignored.
For instance, when calculating transferred turbine torque, the relation between transferred pump torque and transferred turbine torque is only based on the steady-state look-up table. By comparison, the Hrovat & Tobler model simulates even the steady-state performance with calculations based on actual hardware design parameters.

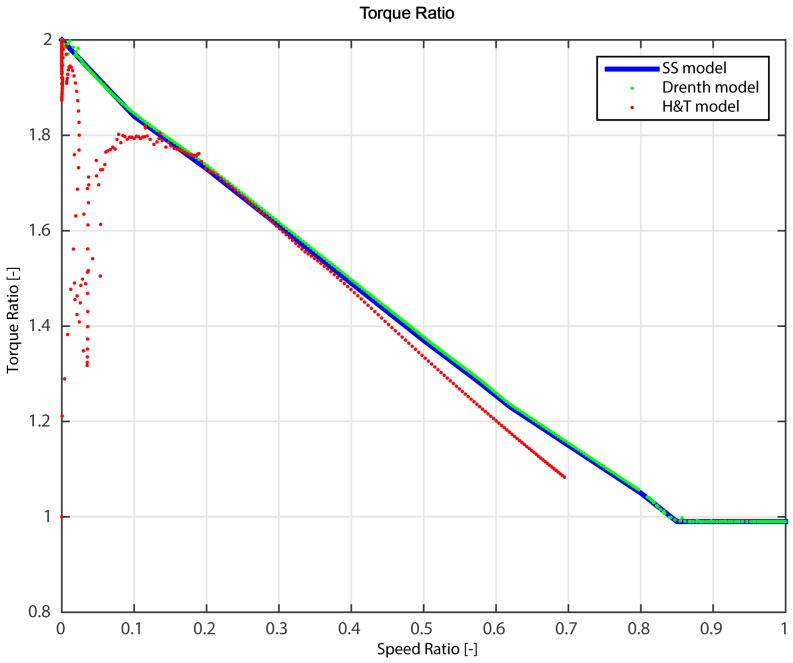

Figure 4.8: Comparison of simulated Torque Ratio.

The models show a clear difference in Torque Ratio at low speed ratios which is due to the different modelling approaches. The drop in Torque Ratio at low speed ratios, seen in the Hrovat & Tobler model, is due to fluid dynamics. The Drenth model does not capture this fast transient and this can also be seen in Figures 4.1 and 4.3. The difference in Torque Ratio above $SR \approx 0.40$ is covered in Section 3.2.1.

4.2.3 Summary of the dynamic models

Compared to the Hrovat & Tobler model, the Drenth model has less complexity, which means faster simulation times, but still provides high accuracy during the tests performed. Since it is based on performance measurements of an existing converter it can not be used to analyse design changes and new concepts. The Hrovat & Tobler model is far more complex and since it is based on hardware design parameters has the potential to be used for evaluating design changes and new concepts, all though it may not be highly accurate for reasons discussed in Section 4.2.1 above. It should also be noted that some parameters, such as loss coefficients, can not be measured or calculated. In this thesis these parameters were obtained by matching the models performance to data obtained from the torque converters manufacturer.

These parameters are highly dependant on the design of the converter, so in order to implement the model for a design concept (when no performance measurements are available for parameter matching) it is likely necessary to first obtain a deeper understanding of how different designs tend to influence these parameters, so that they can be estimated.

4.3 Other possible reasons for simulation inaccuracies

As previously seen, there are some differences between simulated results and measurements. In the previous sections some theoretical sources of error, based on the models themselves were discussed. There are however other factors that can affect the results, and these are presented and discussed below.

4.3.1 Internal torque build-up in AWD drivelines

Both in the rig test and in the in-vehicle measurements, an AWD driveline was used. When the gearbox is in drive and the vehicle is held stationary by application of the brakes, internal torques will build up in the driveline. This is especially true for an AWD vehicle. These internal torques are released when the vehicle starts to roll and may be part of the comparatively large deviations between simulation results and measurement during the first ~0.1 seconds as seen in some of the measurements.

4.3.2 Influence of input torque

During the matching of the Hrovat & Tobler model to manufacturer data it was found that the simulation results could only be matched if some of the blade angles were outside the measured ranges. It was suspected that the method used and described in Section 3.2.1 (input a fixed impeller speed and varying the turbine speed to cover speed ratios from 0 to 1) was not suitable for this type of testing and that this might be the reason the results could not match. It was found that the input torque level can affect the Capacity Factor to a significant degree [9], but the Hrovat & Tobler model does not capture this behaviour. Furthermore, the documentation provided by the manufacturer does not specify the method of measurement. Standards for torque converter performance measurements (SAE J643 and JASO C201) were studied and based on this it is suspected that the provided measurements were performed at a high input torque level, but this is not verified.

Results from Kietlinski and Fingerman (2007) show that the Capacity Factor drops for low speed ratios when input torque is increased [9]. This behaviour is illustrated by the figure below.

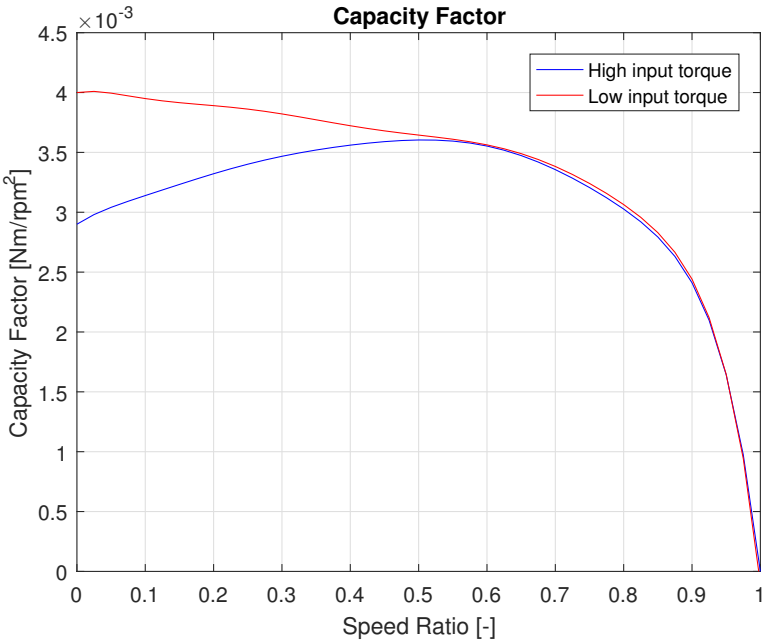

Figure 4.9: Input torque effect on Capacity Factor. (Generic plot for illustration).

It is also concluded that this effect is more severe with a more squashed converter [9]. The torque converter analysed by Kietlinsky and Fingerman had a squash-ratio of 20 %, meaning that the width of the flow path is 80 % of its height, as illustrated in Figure 2.5. The converters studied in this thesis have a squash-ratio of approximately 35 %, which should make this effect even more severe. When comparing the manufacturers Capacity Factor data in Figure 3.4 to the trends illustrated in Figure 4.9 it also seems likely that the tests were performed at high input torque. If the blade angles in the model were kept within reasonable values (based on the converter measurements) the Capacity Factor curve attained by simulation would not drop at low speed ratios and showed a very high resemblance with the "Low input torque" curve in Figure 4.9. This result is also coherent with the findings of Kietlinski and Fingerman [9].
Since this was the only data available for verification it was necessary to accept this discrepancy and allow the blade angles to be outside the measured range.

It should also be noted that this behaviour will likely affect all the models, since this indicates that the measured steady-state characteristics are only valid for the input torque at which the measurements are performed.

4.3.3 Measurement errors

Errors at the turbine side in the complete vehicle level simulations can originate from errors transferred from the pump side. As can be seen in Figures 3.16 and 3.18, there is a significant difference in the effective pump input torque between simulation and measurement. According to Equation 3.1, effective pump input torque is calculated by subtracting pump inertia effects from the engine crankshaft torque. In the equation, the crankshaft torque and the pump inertia are the same between simulation and measurement. This means that the difference in effective pump input torque is caused by the difference in pump speed and acceleration. The difference in pump speed between the three different models and the measured data is presented below.

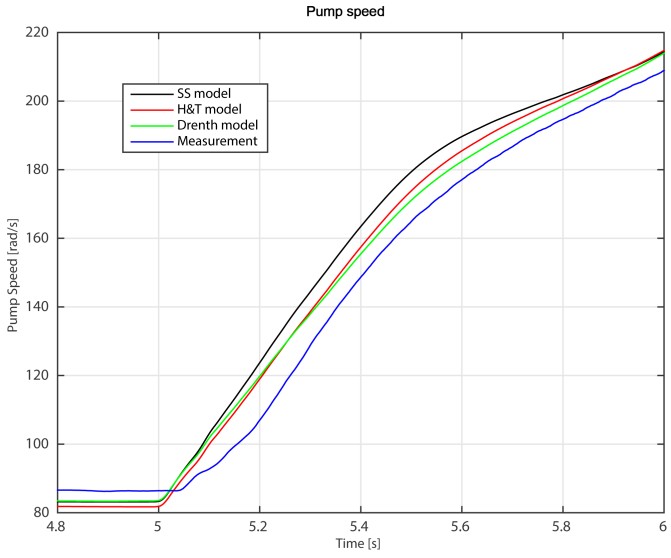

Figure 4.10: Pump speed, simulation and measurement data.

As can be seen from Figure 4.10, the pump speed differs between the three models and the measurement data, which causes a difference in pump acceleration and hence the difference in effective pump torque during the first ~0.2 seconds. Part of the difference is also caused by the sensor used during the measurements, since the speed signal is not picked up instantly.

5
Conclusion

In this project, a simple steady-state based torque converter model was evaluated against two dynamic models of varying complexity. The results indicate that the two dynamic models were both able to capture transient characteristics during vehicle take-off, while also showing satisfactory results under steady-state conditions.
The dynamic models were more time-consuming to implement, in general less robust and gave longer simulation times when compared to the steady-state model. They do however have the capability to capture transient dynamics, which is a necessity when simulating scenarios such as vehicle take-off and hard accelerations. From the analysis of the dynamic models, it was found that the shape effect factor had the largest influence on the torque converters transient performance. A converter with a small shape effect is less sensitive to transients, and performs closer to the steady-state measurements.
The Hrovat & Tobler model was able to capture faster transients than the Drenth model, which suggests that it may be more suitable for analysing the early phases of acceleration, typically the first tenths of a second. The Drenth model was less accurate during the earliest phases of fast transients, but in general works well for acceleration simulation.
The torque converter is a complex component to design since its performance is based on highly complex, three-dimensional fluid flow that changes significantly over the operating range. Effectively no design parameter, such as a radius or a blade angle or blade profile can be changed individually without affecting the fluid flow and hence the interaction with the other elements inside the converter. Trade-offs are always required during the design process in order to achieve the most beneficial parametrisation for each application.

5.1 Future work

In Section 4.2.1 it was concluded that the Hrovat & Tobler model assumes that the flow path inside the converter is perfectly circular and that it therefore may not be suitable for simulating highly squashed converters. As shown and discussed in Chapter 4, the shape effect factor has the largest effect on the effective torque transfer during transients. By examining Equation 2.12 and 2.13 it is clear that the modelling of the fluid dynamic component is quite rudimentary. As a scope for future work, it is therefore suggested that the modelling of the fluid dynamic component could be developed. Our suggestion is to replace or elaborate the shape effect factor in an attempt to take the level of converter squash into account.

Bibliography

[1] Fluid Coupling (2010). In *Encyclopaedia Britannica Online* [online]. Retrieved from `http://www.britannica.com` on May 2, 2016.

[2] T. Yamaguchi and K. Tanaka (2012). Torque converter transient characteristics prediction using computational fluid dynamics. *IOP Conference Series: Earth and Environmental Science, Volume 15, Part 4.* Page 9.

[3] C. Liu, C. Liu and W. Ma (2015). Mathematical Model for Elliptic Torus of Automotive Torque Converter and Fundamental Analysis of Its Effect on Performance. *Mathematical Problems in Engineering, Volume 2015, Article ID 851816.*

[4] R. H. Barnard (2001). Automotive engineering development. In: J. Happian-Smith, editor *An Introduction to Modern Vehicle Design*, 1st edition. Woburn: Butterworth-Heinemann. Page 20.

[5] N. Vaughan and D. Simner (2001). Transmissions and driveline. In: J. Happian-Smith, editor *An Introduction to Modern Vehicle Design*, 1st edition. Woburn: Butterworth-Heinemann. Page 428.

[6] D. Maddock (2015). Automotive Torque Converters. In: D. Crolla, D. E. Foster, T. Kobayashi and N. Vaughan, editors-in-chief *Encyclopedia of Automotive Engineering*, 1st edition. Chichester: John Wiley & Sons Ltd.

[7] D. Hrovat and W. E. Tobler (1985). Bond graph modelling and computer simulation of automotive torque converters. *Journal of the Franklin Institute*, Vol. 319, No. 1/2, Page 93-114.

[8] B. Pohl (2003). Transient Torque Converter Performance, Testing, Simulation and Reverse Engineering. *SAE Technical Paper 2003-01-0249.* [online]. Retrieved from `http://papers.sae.org/2003-01-0249/` on February 26, 2016.

[9] T. Kietlinski and M. Fingerman (2007). 248mm Elliptical Torque Converter from DaimlerChrysler Corporation. *SAE Technical Paper 2007-01-0241.* [online]. Retrieved from `http://papers.sae.org/2007-01-0241/` on March 15, 2016.

[10] E. Drenth (2012). Dynamics of Torque Converter. *Modelon AB, document number MVD20120505/5, reference MVD20120208.* [Confidential].

A

Appendix - Nomenclature

I_p = Pump inertia $[kg \cdot m^2]$
I_t = Turbine inertia $[kg \cdot m^2]$
I_s = Stator inertia $[kg \cdot m^2]$
ρ = Fluid density $[kg/m^3]$
A = Flow path area $[m^2]$
r_p = Pump exit radius $[m]$
r_t = Turbine exit radius $[m]$
r_s = Stator exit radius $[m]$
L_f = Equivalent fluid length $[m]$
α_p = Pump exit angle [°]
α_t = Turbine exit angle [°]
α_s = Stator exit angle [°]
α_{pp} = Pump inlet angle [°]
α_{tt} = Turbine inlet angle [°]
α_{ss} = Stator inlet angle [°]
$C_{sh,p}$ = Pump shock loss coefficient [-]
$C_{sh,t}$= Turbine shock loss coefficient [-]
$C_{sh,s}$= Stator shock loss coefficient [-]
f = Friction loss coefficient [-]
S_p = Shape effect of pump $[m]$
S_t = Shape effect of turbine $[m]$
S_s = Shape effect of stator $[m]$
m_p = Fluid mass in pump $[kg]$
m_t = Fluid mass in turbine $[kg]$
m = Total fluid mass in converter $[kg]$

B

Appendix - Geometrical parameters for the Hrovat & Tobler model

This appendix illustrates the dimensions and angles specified in the Hrovat & Tobler simulation model.
The model assumes that the working fluid follows a mean path inside the torque converter. Interaction between the impeller, turbine and stator is calculated based on the radii and angles at which the fluid exits one element and enters the next.

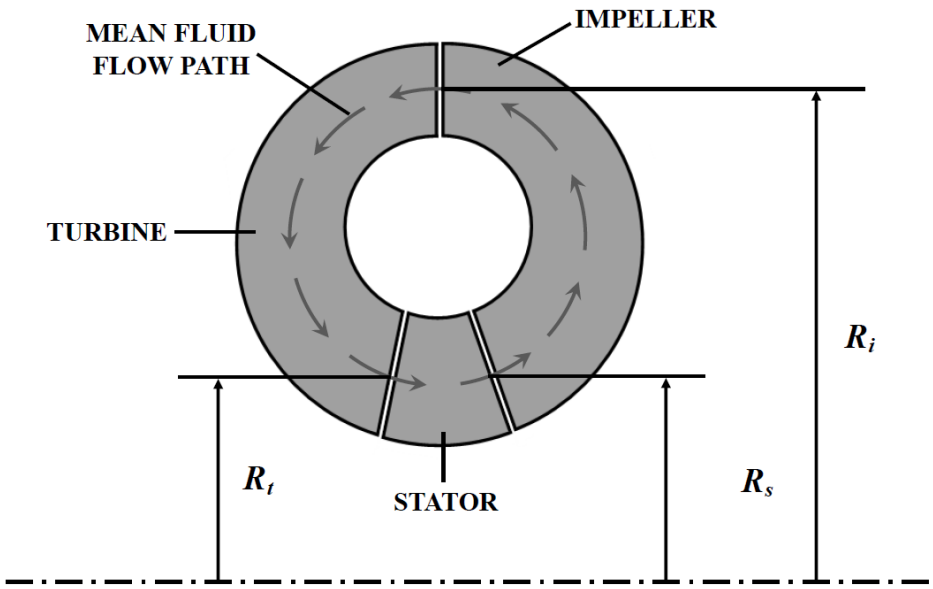

Figure B.1: Radii at impeller, turbine and stator exits

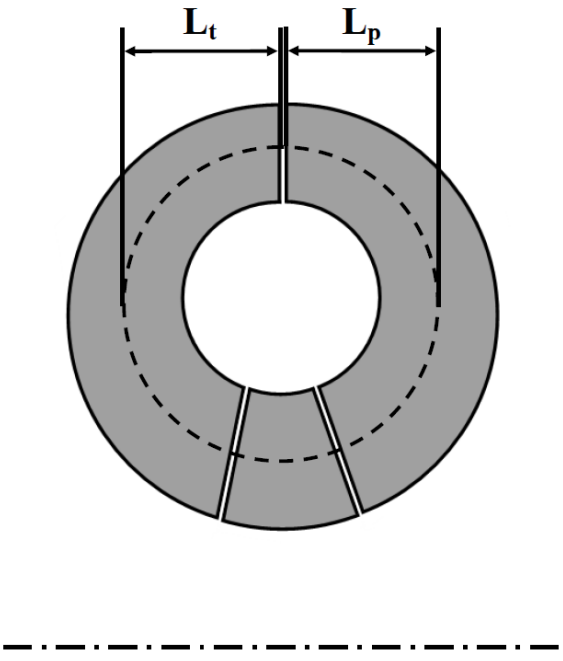

Figure B.2: Axial projections of meridian streamlines

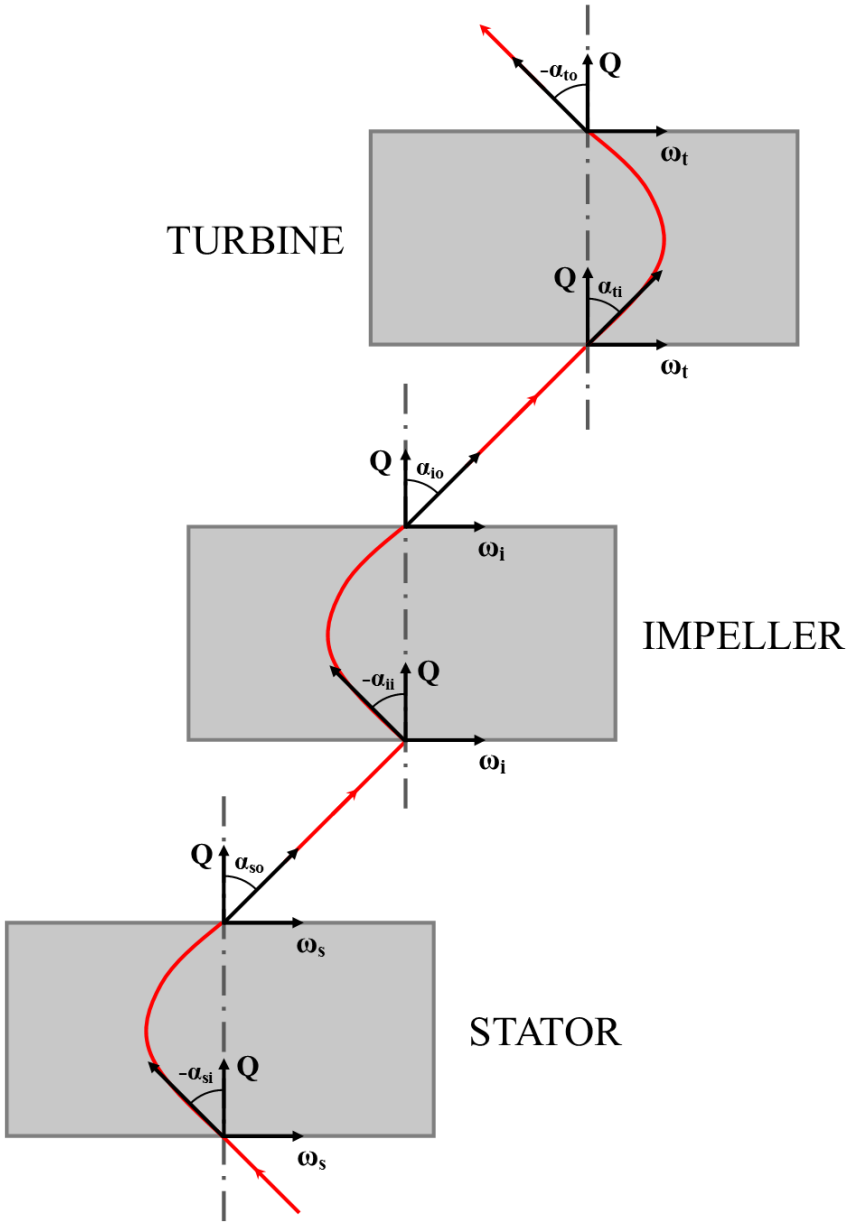

Figure B.3: Blade angles for impeller, turbine and stator inlets and outlets

In the above figure, Q is the volume flow of the working fluid, ω is rotational speed and α is the blade angle. The first index defines the element (i for impeller, t for turbine or s for stator) and the second index denotes i for inlet and o for outlet. For instance ω_i for 'Rotational speed, impeller', α_{si} for 'Blade angle, stator inlet' and α_{io} for 'Blade angle, impeller outlet'.

C

Appendix - Example of steady-state look-up table

Due to confidentiality the steady-state look-up tables for the torque converters studied in this thesis can not be presented. The table and graphs shown below are examples for illustrational purposes. For this particular converter the coupling point is reached at SR=0.85.

Table C.1: Example of steady-state look-up table.

Speed Ratio [−]	**Torque Ratio** [−]	**Capacity Factor** $[Nm \cdot 10^{-3}/rpm^2]$
0.00	2.14	3.272
0.10	1.99	3.257
0.20	1.84	3.228
0.30	1.70	3.181
0.40	1.56	3.112
0.50	1.43	3.017
0.60	1.30	2.887
0.70	1.18	2.713
0.80	1.06	2.481
0.85	1.00	2.370
0.90	1.00	1.842
0.95	1.00	1.237
1.00	1.00	0.187

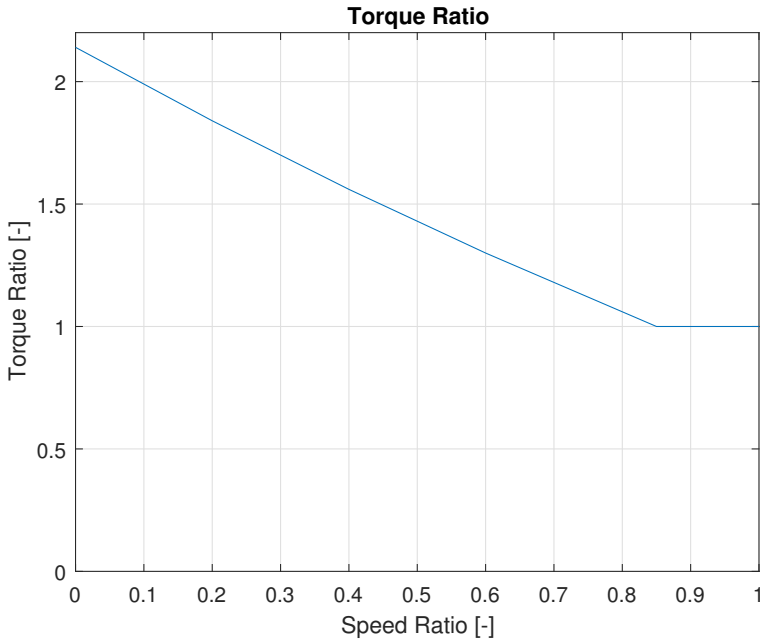

Figure C.1: Graph of steady-state Torque Ratio.

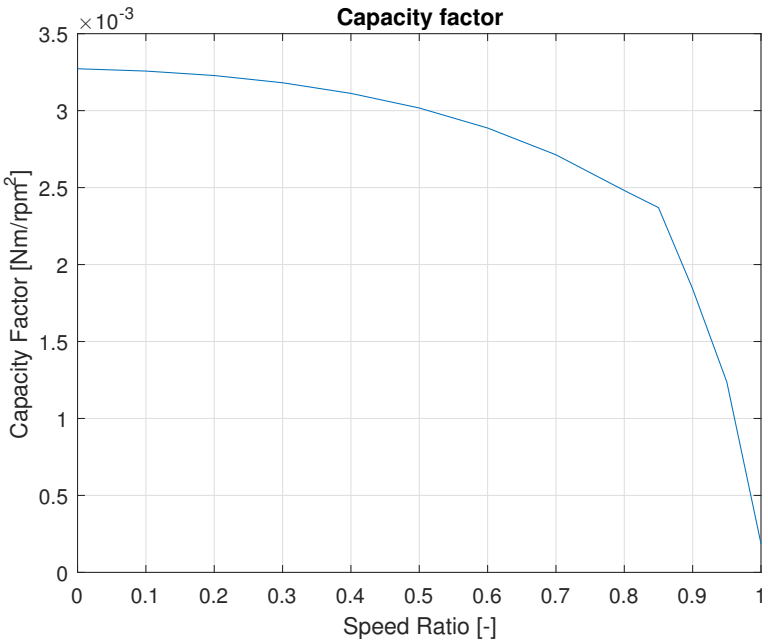

Figure C.2: Graph of steady-state Capacity Factor.

D

Appendix - Parameter study

This appendix contains graphs from a parameter study of the Hrovat & Tobler model. The impeller speed was held constant at 2,000 rpm while the turbine speed was controlled by sweeping the Speed Ratio from 0 to 0.9 with increments of 0.05. The model was run until stable, i.e. steady-state was reached.
The table below lists the input parameters, reference values and the ranges used for the study. Only one parameter was changed during each run, the others were kept at their respective reference values.
Please note that the range and scale of the vertical axis is different in some of the Capacity Factor and Volume Flow graphs.

Table D.1: Parameters used for parameter study

Parameter [$unit$]	Reference value	Range
Flow area [m^3]	0.01	Reference ±25%
Fluid density [kg/m^3]	840	800 - 900
Impeller exit radius [m]	0.12	Reference ±25%
Turbine exit radius [m]	0.065	Reference ±25%
Stator exit radius [m]	0.06	Reference ±25%
Impeller exit angle [°]	-20	-60 - 60
Turbine exit angle [°]	-50	-60 - 60
Stator exit angle [°]	60	-60 - 60
Impeller inlet angle [°]	-50	-60 - 60
Turbine inlet angle [°]	55	-60 - 60
Stator inlet angle [°]	15	-60 - 60
Impeller shock-loss coefficient [-]	1	Reference ±50%
Turbine shock-loss coefficient [-]	1	Reference ±50%
Stator shock-loss coefficient [-]	1	Reference ±50%
Fluid friction factor [-]	0.2	0.2-0.8

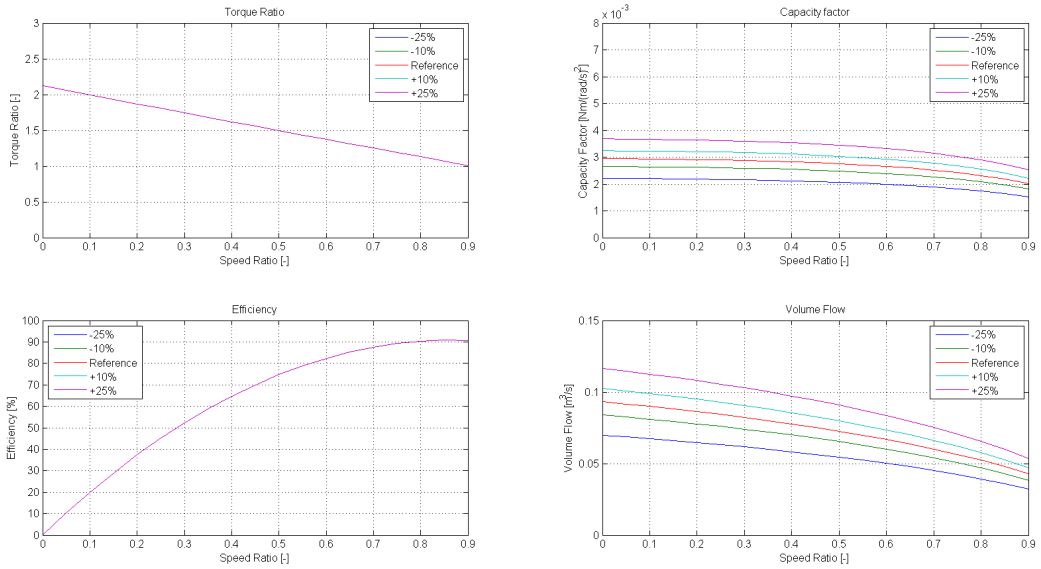

Figure D.1: Effect of parameter 'Fluid area'

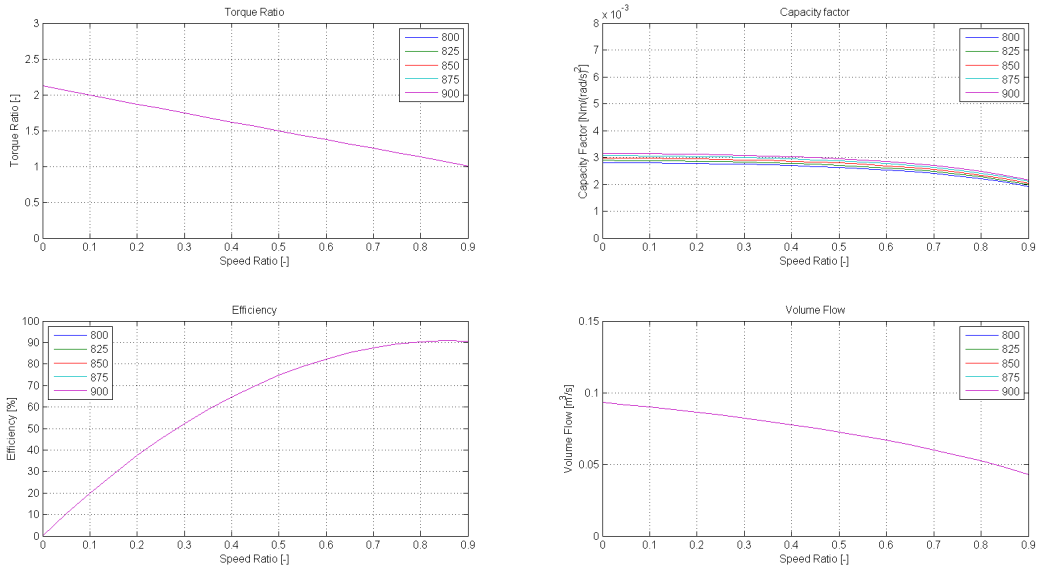

Figure D.2: Effect of parameter 'Fluid density'

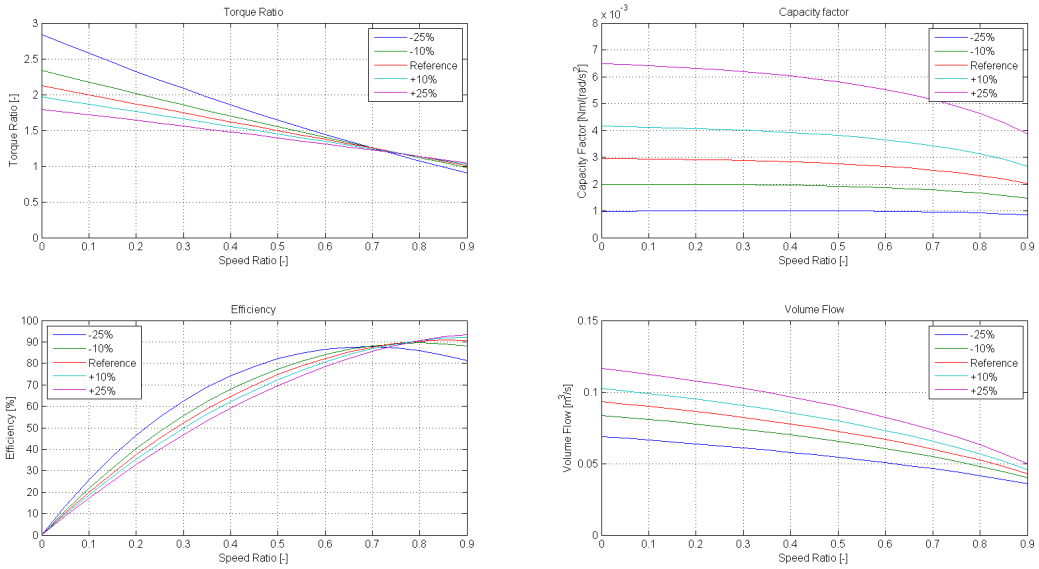

Figure D.3: Effect of parameter 'Impeller exit radius'

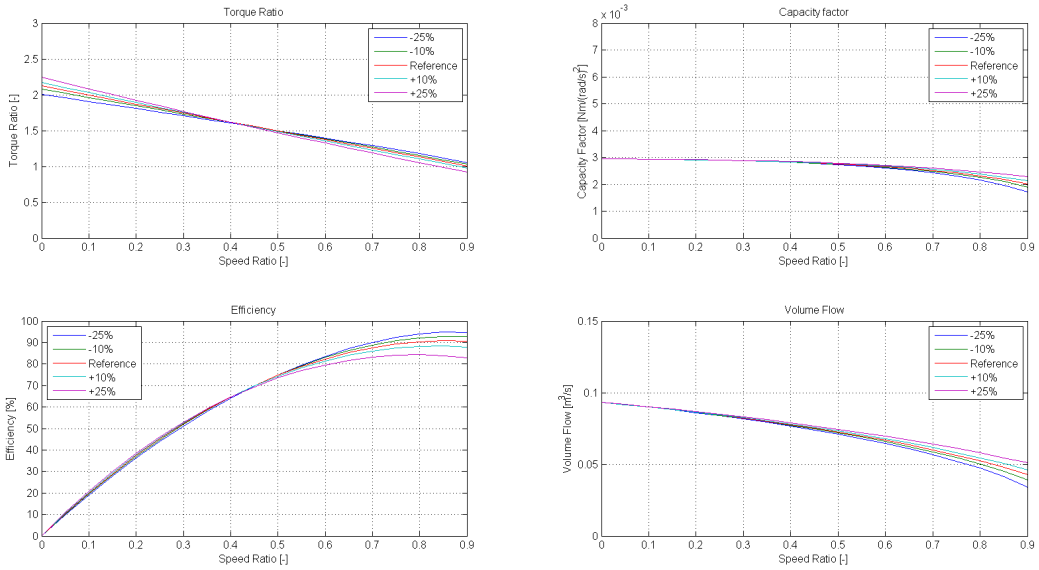

Figure D.4: Effect of parameter 'Turbine exit radius'

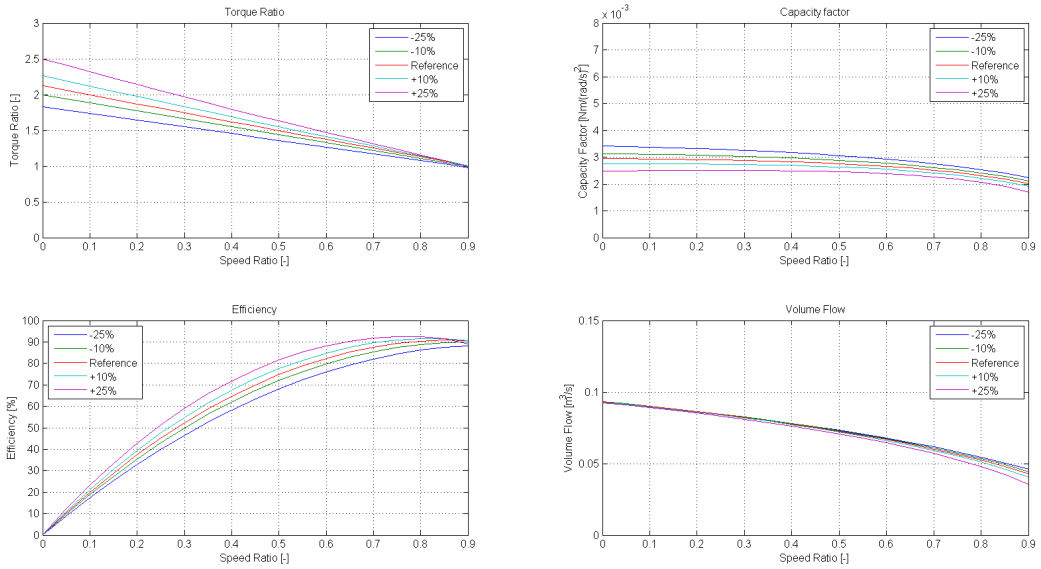

Figure D.5: Effect of parameter 'Stator exit radius'

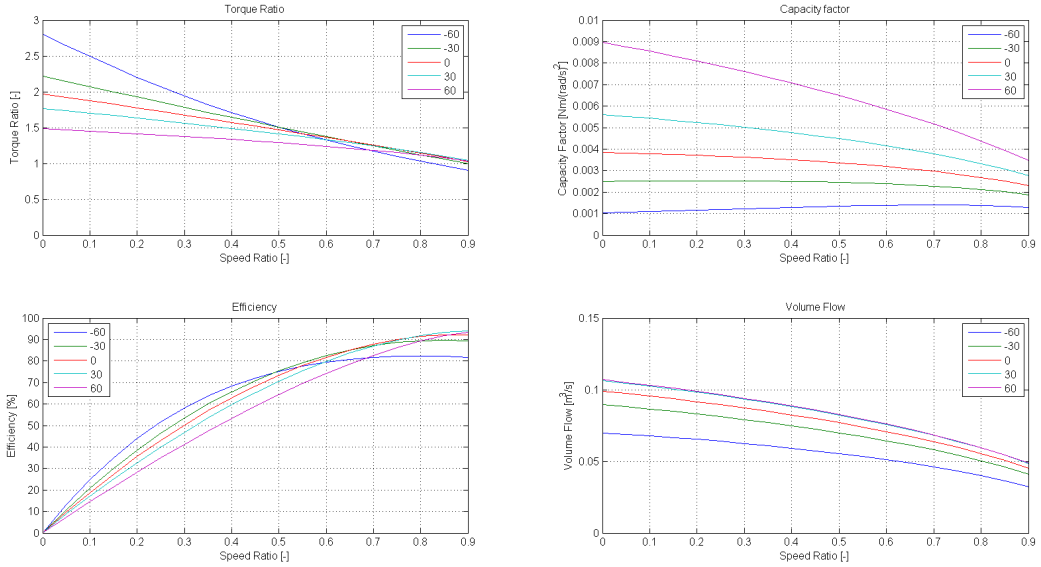

Figure D.6: Effect of parameter 'Impeller exit angle'

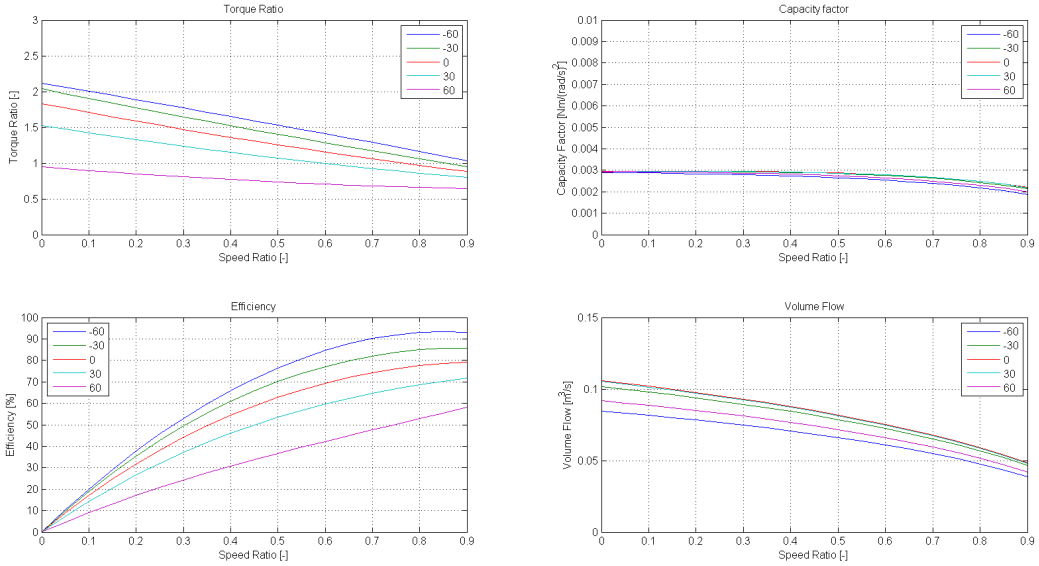

Figure D.7: Effect of parameter 'Turbine exit angle'

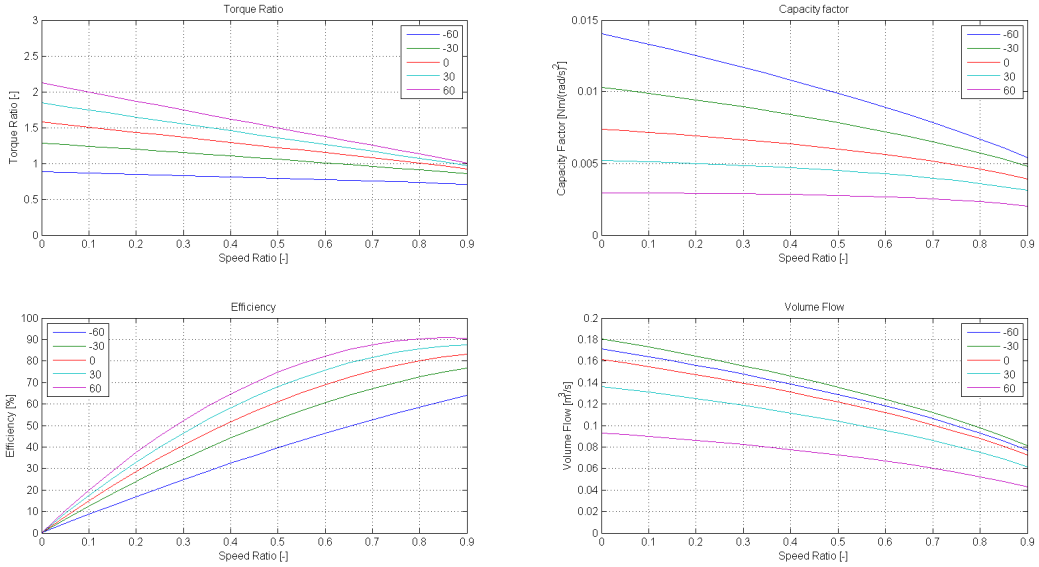

Figure D.8: Effect of parameter 'Stator exit angle'

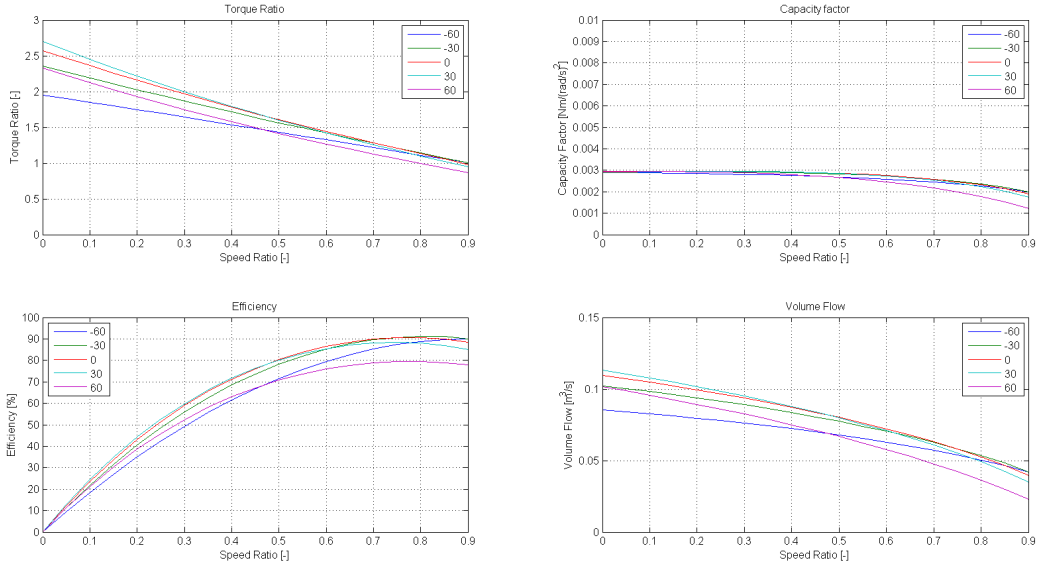

Figure D.9: Effect of parameter 'Impeller inlet angle'

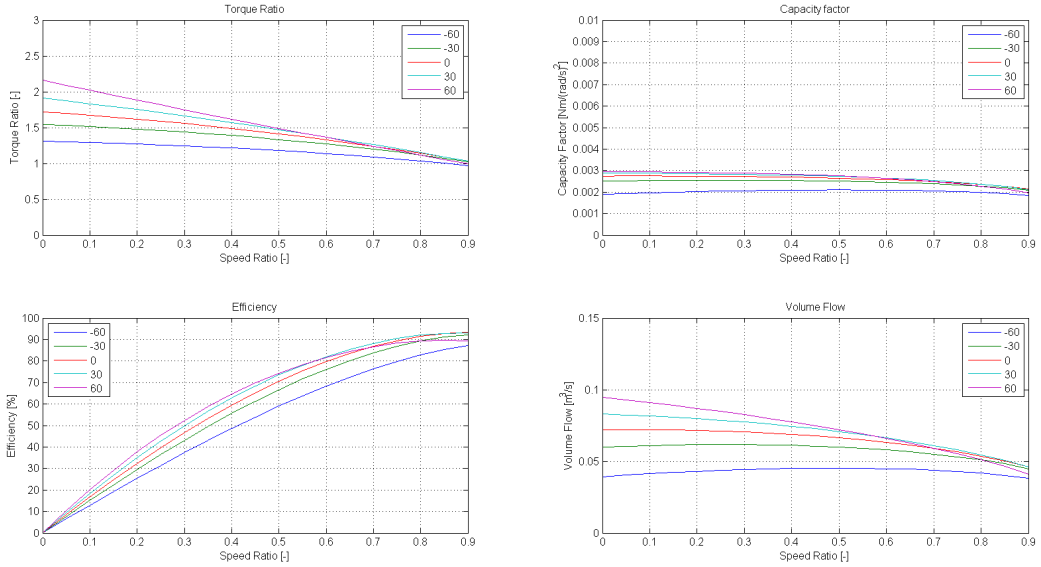

Figure D.10: Effect of parameter 'Turbine inlet angle'

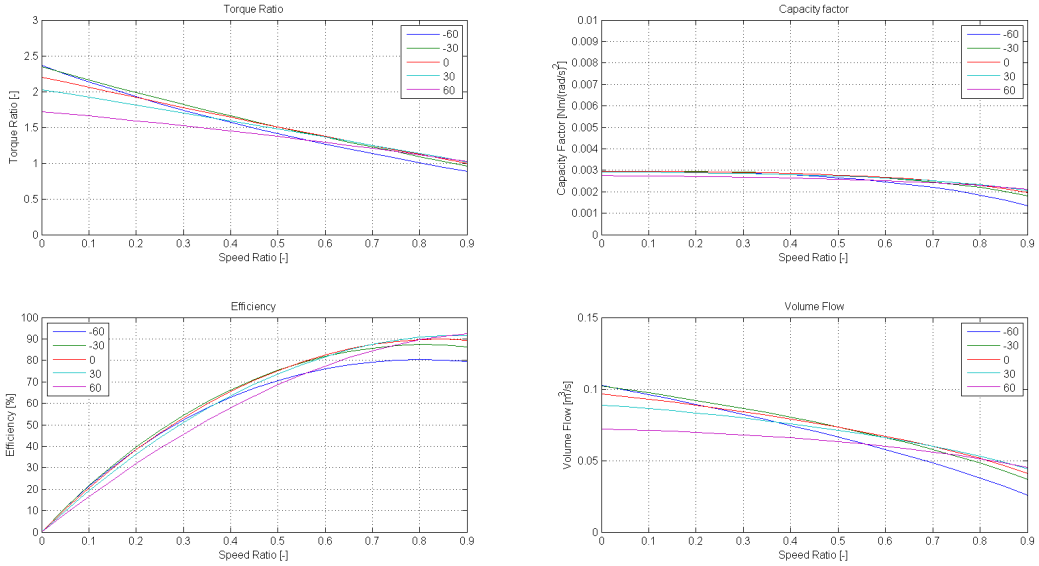

Figure D.11: Effect of parameter 'Stator inlet angle'

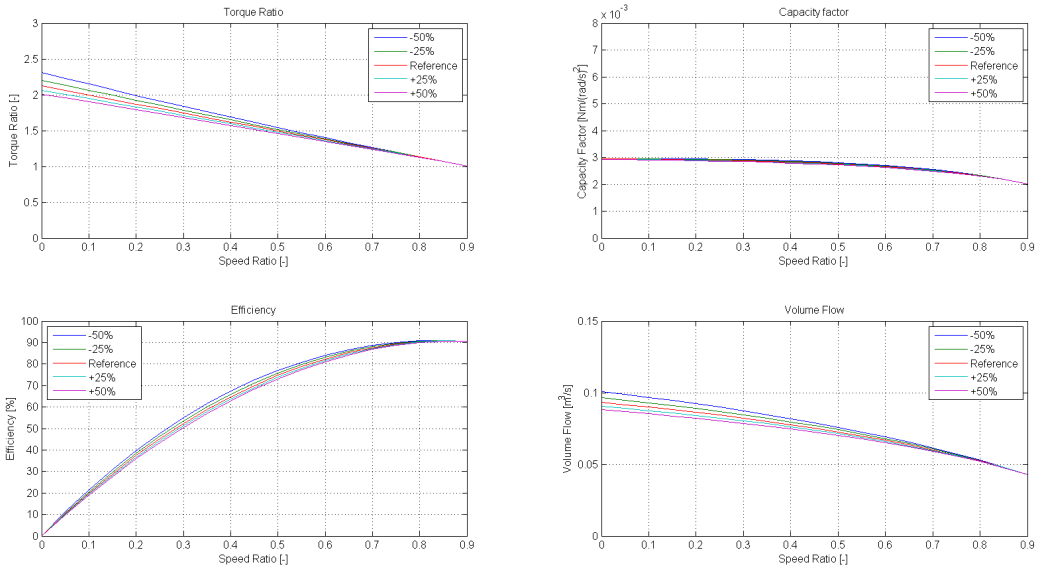

Figure D.12: Effect of parameter 'Impeller shock-loss coefficient'

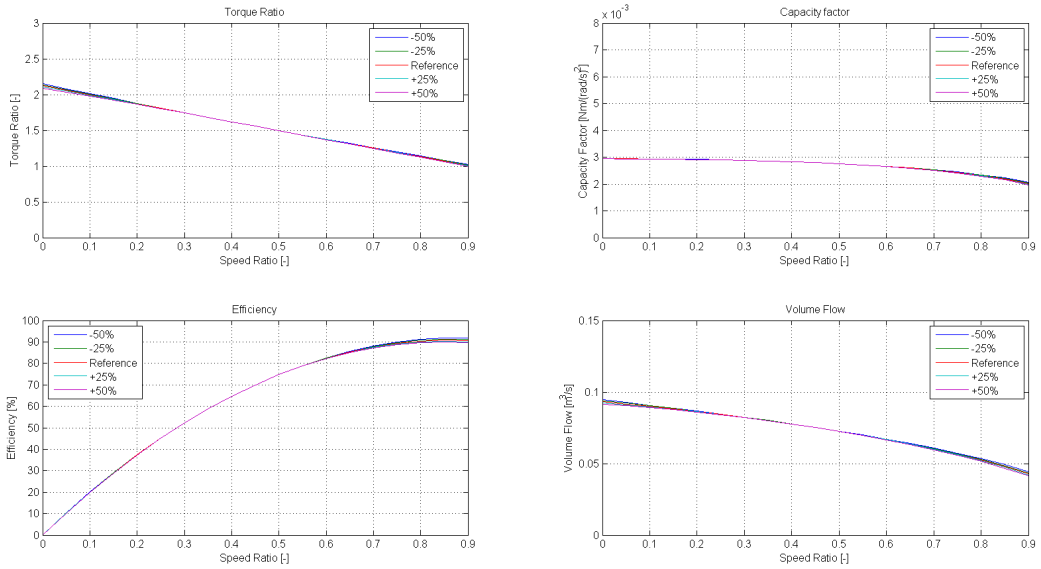

Figure D.13: Effect of parameter 'Turbine shock-loss coefficient'

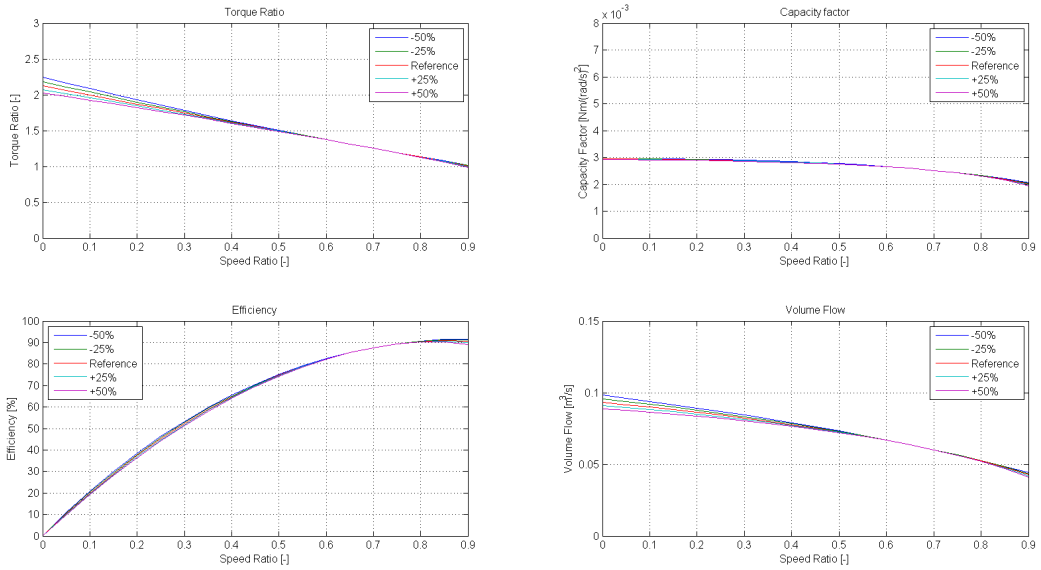

Figure D.14: Effect of parameter 'Stator shock-loss coefficient'

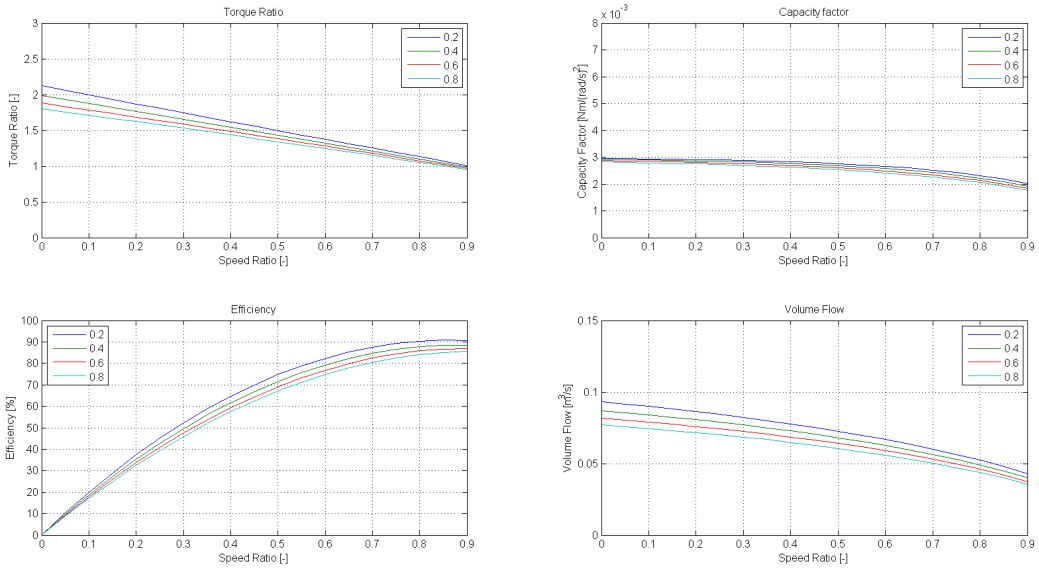

Figure D.15: Effect of parameter 'Fluid friction factor'